J. Fluid Mech. (1988), *vol.* 189, *pp.* 53–86
Printed in Great Britain

Three-dimensional instability of a plane free shear layer: an experimental study of the formation and evolution of streamwise vortices

By J. C. LASHERAS AND H. CHOI
Department of Mechanical Engineering, University of Southern California, Los Angeles, CA 90089-1453, USA

(Received 10 November 1986 and in revised form 24 July 1987)

The three-dimensional development of a plane free shear layer subjected to small sinusoidal perturbations periodically placed along the span is experimentally studied. Both laser induced fluorescence and direct interface visualization are used to monitor the interface between the two fluids. The development of the different flow stabilities is obtained through analysis of the temporal and spatial evolution of the interface separating the two streams. It is shown that the characteristic time of growth of the two-dimensional shear instability is much shorter than that of the three-dimensional instability. The primary Kelvin–Helmholtz instability develops first, leading to the formation of an almost two-dimensional array of spanwise vortex tubes. Under the effect of the strain field created by the evolving spanwise vortices, the perturbed vorticity existing on the braids undergoes axial stretching, resulting in the formation of vortex tubes whose axes are aligned with the principal direction of the positive strain field. During the formation of these streamwise vortex tubes, the spanwise vortices maintain, to a great extent, their two-dimensionality, suggesting an almost uncoupled development of both instabilities. The vortex tubes formed through the three-dimensional instability of the braids further undergo nonlinear interactions with the spanwise vortices inducing on their cores a wavy undulation of the same wavelength, but 180° phase shifted with respect to the perturbation. In addition, it is shown that owing to the nature of the three-dimensional instability, the effect of vertical and axial perturbations are coupled. Finally, the influence of the amplitude and wavelength of the perturbation on the development of the two- and three-dimensional instabilities is described.

1. Introduction

In a plane free shear layer, large-scale spanwise vortices have been observed forming at a wide variety of Reynolds numbers (Brown & Roshko 1971, 1974; Rebollo 1973; Winant & Browand 1974; Dimotakis & Brown 1976). These two-dimensional vortices are the result of the Kelvin–Helmholtz shear instability. In addition to the primary two-dimensional vortical structure, it has long been observed that the plane free shear layer also contains a well-organized array of streamwise vortices that superimpose onto the spanwise eddies. The presence of this secondary structure was observed by Konrad (1976) and later by Breidenthal (1978, 1981) and Jimenez (1983), among others. However, not until recently did Bernal (1981) present conclusive evidence that the streamwise streaks (previously observed in the plane views of the gas and liquid mixing layers of Konrad and Breidenthal)

were actual counter-rotating pairs of axial vortices superimposed onto the spanwise structure. Jimenez, Cogollos & Bernal (1985) through a three-dimensional reconstruction via digital image processing of motion pictures of a plane turbulent mixing layer confirmed Bernal's findings. Their three-dimensional graphics reconstruction shows that after the transition to three-dimensionality, the mixing layer exhibits an array of counter-rotating pairs of streamwise vortices. Recently, Lasheras, Cho & Maxworthy (1986) showed that the plane, free shear layer is unstable to three-dimensional perturbations in the upstream conditions. This instability was found to result in the formation of a well-organized array of streamwise vortices on the braids between consecutive spanwise vortices. Depending on the location and the magnitude of the disturbances, it was found that the position where the streamwise vortices form changes substantially. Furthermore, the results of Lasheras *et al.* (1986) show that under the effect of the strain field created by the spanwise vortices, small localized upstream disturbances spread laterally by strong self-induction resulting in the sideways formation of counter-rotating pairs of streamwise vortices.

Several theoretical predictions have been made about the formation of these streamwise vortices, (Corcos 1979; Corcos & Lin 1984; Lin & Corcos 1984; Pierrehumbert & Widnall 1982). Furthermore, the formation of these streamwise vortices has also been detected in recent numerical calculations using spectral methods (Metcalfe *et al.* 1987) and three-dimensional inviscid vortex dynamics methods (Ashurst & Meiburg 1988). Corcos and co-authors studied the evolution of a row of weak alternating vortices with axes parallel to the direction of a uniform positive strain field. Their calculations indicate that the streamwise vorticity introduced into the shear layer is stretched on the braids between consecutive spanwise vortices under the positive strain existing in the region. These numerical calculations show that for certain values of the strain and distance between axial vortices, the streamwise vorticity may develop into concentrated, round vortices. Pierrehumbert & Widnall, through a linear instability analysis of a family of coherent Stuart vortices (to simulate the array of spanwise eddies) suggested that the streamwise vortices could be the result of a translative instability of these arrays of vortices.

Although the above theories provide possible mechanisms for the generation of streamwise vortices, the origin and the evolution of this three-dimensional motion have not yet been corroborated experimentally. In this paper, we will study experimentally a plane free shear layer subjected to perturbations periodically placed along the span. By analysing the evolution of the vorticity field, we will determine the development of the different instabilities occurring in the flow. In particular, we will focus our study on the three-dimensional instability leading to the formation of the streamwise vortices. The experimental results will then be used to check the different theories.

Section 2 describes the experimental techniques. The experimental results corresponding to a representative case in which the plane free shear layer is subjected to a single-wave, horizontal, spanwise disturbance is presented in §3. The mechanism for the three-dimensional instability which leads to the formation of streamwise vortex tubes is discussed in §4. Section 5 describes the effect of the orientation, wavelength, and amplitude of the perturbation. In §7, the so-called 'natural' case where the base flow is subjected to uncontrolled small random disturbances is discussed. Conclusions are given in §8.

2.1. *Experimental facility and flow conditions*

Our previous experimental results (Lasheras *et al.* 1986) show that the plane mixing layer is extremely sensitive to small random upstream disturbances; however, they also show that in the absence of perturbations, the layer can remain two-dimensional, even five to six wavelengths downstream of its origin. Consequently, to analyse the stability of a plane free shear layer to several types of perturbations, we designed an experimental facility in which extreme care was taken to minimize the presence of small uncontrolled random disturbances. Under these conditions, the flow facility was able to produce a two-dimensional unperturbed base-flow to which controlled perturbations could be added.

The facility, schematically shown in figure 1, consisted of a blow-down water channel where two horizontal, laminar water streams were formed, initially separated by a flat plate. At the trailing edge of the splitter plate, the two streams were allowed to meet and to mix in a 2 m long test section. The test rig was a modified version of the one previously used in our mixing-layer experiments described in Lasheras *et al.* 1986. The two laminar flows were created in an 80 cm long settling chamber formed by layers of sponges, honeycomb, and fine mesh screens. This was followed by a fifth-order polynomial, three-dimensional, 40 cm long, contraction nozzle, with a contraction area ratio of 9:1. The facility operated continuously in a closed loop by recirculating the fluid collected in the dump section back to the supply tanks through pumps.

Several sources of random upstream disturbances leading to the loss of two-dimensionality of the base-flow were identified in our previous experimental work. The most important one was the presence of uncontrolled air bubbles that attached to the screens and solid walls. These air bubbles were a result of dissolved gases and temperature differences. In the present experiments, to reduce the formation of these air bubbles, all the fluids used in each run were kept in large settling tanks for periods of over twenty-four hours, having been filtered and treated by a water-softening unit previously.

Another identified cause of the loss of two-dimensionality in the base-flow was the effect created by the vertical sidewalls of the test section (Lasheras & Maxworthy 1987). As the vorticity of the layer interacted with the vorticity of the walls, we had found that axial vortices were created near the wall region and further induced the sideways formation of additional axial vortex tubes, an effect which propagated towards the centre of the channel. To minimize this shear-layer/wall interaction effect, the test section was designed with a rectangular cross-section 9 cm high × 25 cm wide so that each of the two streams forming the mixing layer had an approximate span to depth ratio of 5:1.

To control the thickness of both boundary layers on the splitter plate, 40 mesh screens were placed at several distances upstream of the trailing edge. With this arrangement, we were able to generate perfectly two-dimensional free shear layers with the velocities of both streams ranging from 0.5 cm/s to 15 cm/s. No measureable three-dimensional disturbances were detected in the base-flow as far as 15–16 cm downstream of the origin of the layer.

The base-flow configuration selected for this study, and used in all the experiments reported here, was the two-dimensional horizontal plane shear layer formed between two laminar water streams with velocities of $U_1 = 3.4$ cm/s and $U_2 = 1.5$ cm/s in the top and bottom flows respectively. At the trailing edge of the splitter plate (the geometrical origin of the mixing layer) the boundary-layer thicknesses were 9 mm and

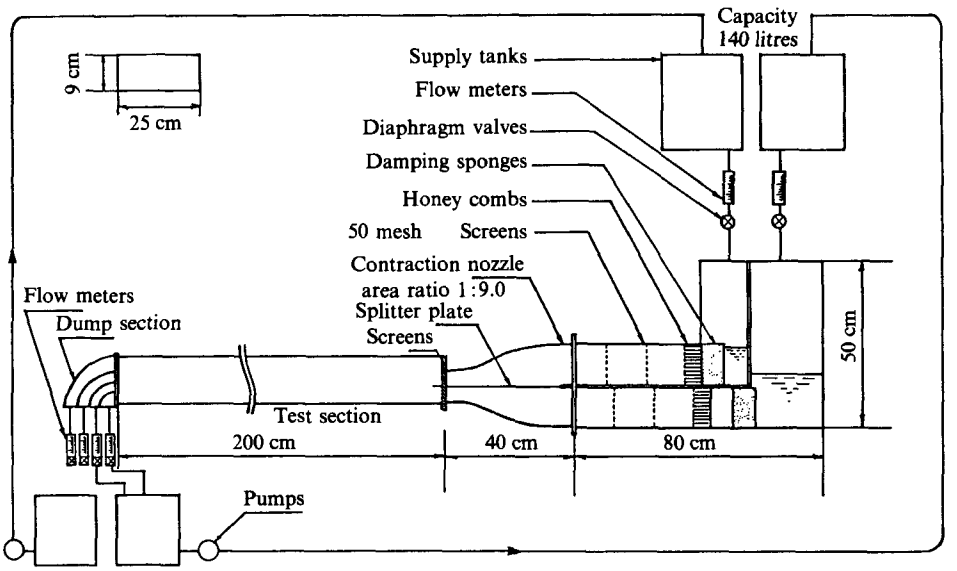

FIGURE 1. Experimental apparatus.

6 mm for the slow and fast streams, while the momentum thicknesses were 0.8 mm and 1.2 mm, respectively. The Reynolds number, based on the velocity difference $(U_1 - U_2)$ and the overall momentum thickness of the layer, was 45 calculated at the geometrical origin of the mixing layer.

2.2. *Perturbations periodically distributed along the span*

Using the above described two-dimensional base-flow, we analysed the response of the plane free shear layer to several types of perturbations periodically distributed along the span. The first type consisted of a single-wave horizontal perturbation in the vorticity sheet emanating from the plate. This was achieved by modifying the trailing edge of the splitter plate to give it a sinusoidal 'indentation' of wavelength λ and amplitude a, (figure 2). The effect of the indentation in the plate was to cause a sinusoidal horizontal displacement of the geometrical origin of the mixing layer, thus producing a periodic axial disturbance in the vortex sheet.

The second type consisted of a single-wave sinusoidal vertical perturbation in the vorticity sheet emanating from the splitter plate. This was achieved by using a modified splitter plate containing a sinusoidal 'corrugation' of wavelength λ and amplitude a (figure 3). The corrugations of the splitter plate caused a sinusoidal vertical (Y) displacement of the geometrical origin of the mixing layer, thus resulting in a periodic vertical perturbation in the vortex sheet.

The third type of perturbation studied consisted of a combined horizontal and vertical wave. By corrugating the indented splitter plate, both the horizontal (X) and vertical (Y) perturbation components were created simultaneously. For this third type, we limited our study to only those cases where the horizontal (indentations) and vertical (corrugations) perturbation components had the same wavelength. Of this combined perturbation, we studied only two cases. The first one consisted of undulating the indented plate so that the tips of the indentations were in phase with the peaks of the corrugations; hereinafter, this case will be referred to as the 'in-phase' case. The second case consisted of having the tips of the indentations in phase

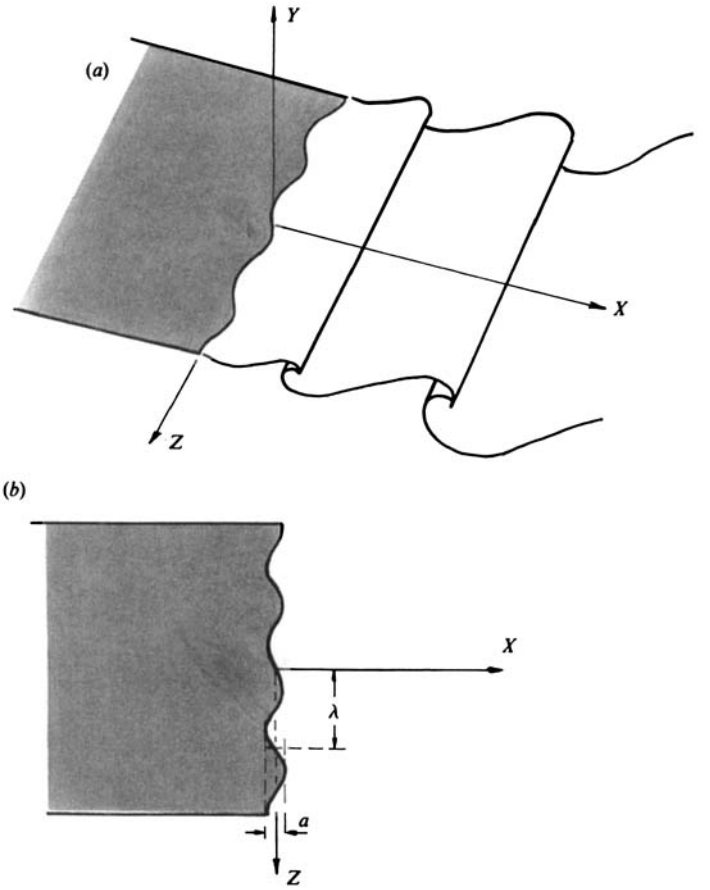

FIGURE 2. Indented splitter plate. (*a*) Perspective view. (*b*) Plan view.

with the valleys of the corrugations. This second one will be referred to as the '180° out-of-phase' case.

To investigate the possible existence of a most unstable wavelength in each of the above mentioned perturbation cases, the wavelength λ was varied systematically from two to ten wavelengths/span (λ = 12.5 cm, 8.3 cm, 6.25 cm, 5 cm, 4.16 cm, 3.57 cm, 3.12 cm, 2.7 cm, and 2.5 cm, respectively). Since, for a given wavelength, the magnitude of the perturbations is directly related to the amplitude of the imposed wave, in all the cases, the amplitude a was kept smaller than the thickness of the boundary layers of the two streams. The amplitude cases studied ranged from a value of 2 mm to 10 mm in 2 mm increments.

2.3. *The flow visualization*

The interface separating both fluids was visualized by using several techniques. The first one consisted of a direct interface visualization (DIV), where the reactive interface was visualized through the use of a pH indicator (Cresol Red). Hydrochloric acid (HCl) and sodium hydroxide (NaOH) water solutions were used in each stream, respectively, to create a reactive interface where the product formation, and thus the interface position, could be detected through the response of the pH indicator. This technique has proved to be a remarkably useful one for the analysis of this type of

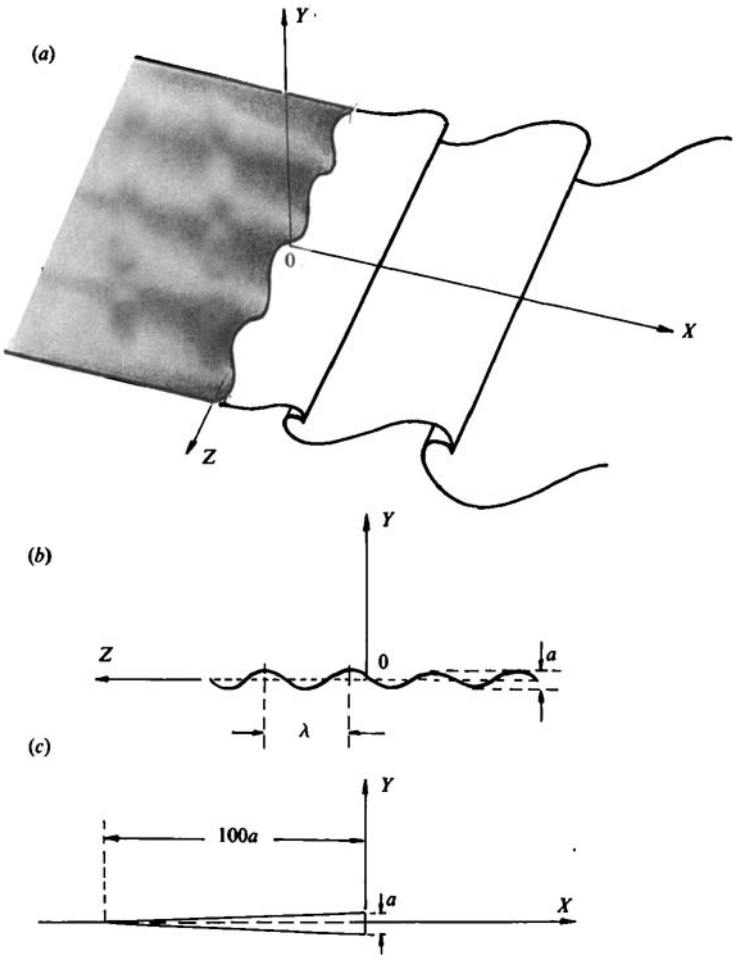

FIGURE 3. Corrugated splitter plate. (*a*) Perspective view. (*b*) End view. (*c*) Side view. The corrugation of wavelength λ and amplitude a is gradually achieved over a length approximately $100a$.

flow (Breindenthal 1978; Lasheras *et al.* 1986). Details of its use can be found in Lasheras *et al.* 1986.

A second technique consisted of using laser induced fluorescence (LIF) to determine the position of the interface by recording the fluorescence induced by a laser plane of fluorescein particles added to one of the streams (Dewey 1976). Finally, a third method consisted of visualizing the interface by inducing the fluorescence of a high concentration of fluorescein particles added to the lower flow with a set of spotlights in order to create a solid opaque effect at the interface. The spotlight arrangement and the fluorescein concentration were selected so that a shadow effect could be created by the corrugated opaque interface, thereby showing its three-dimensionality.

2.4. *Analysis of the features of the flow*

In the ideal case, where the shear layer develops from two streams having infinitesimally small boundary layers, the vorticity in the flow is initially confined to a very narrow region around the interface. When the different instabilities develop

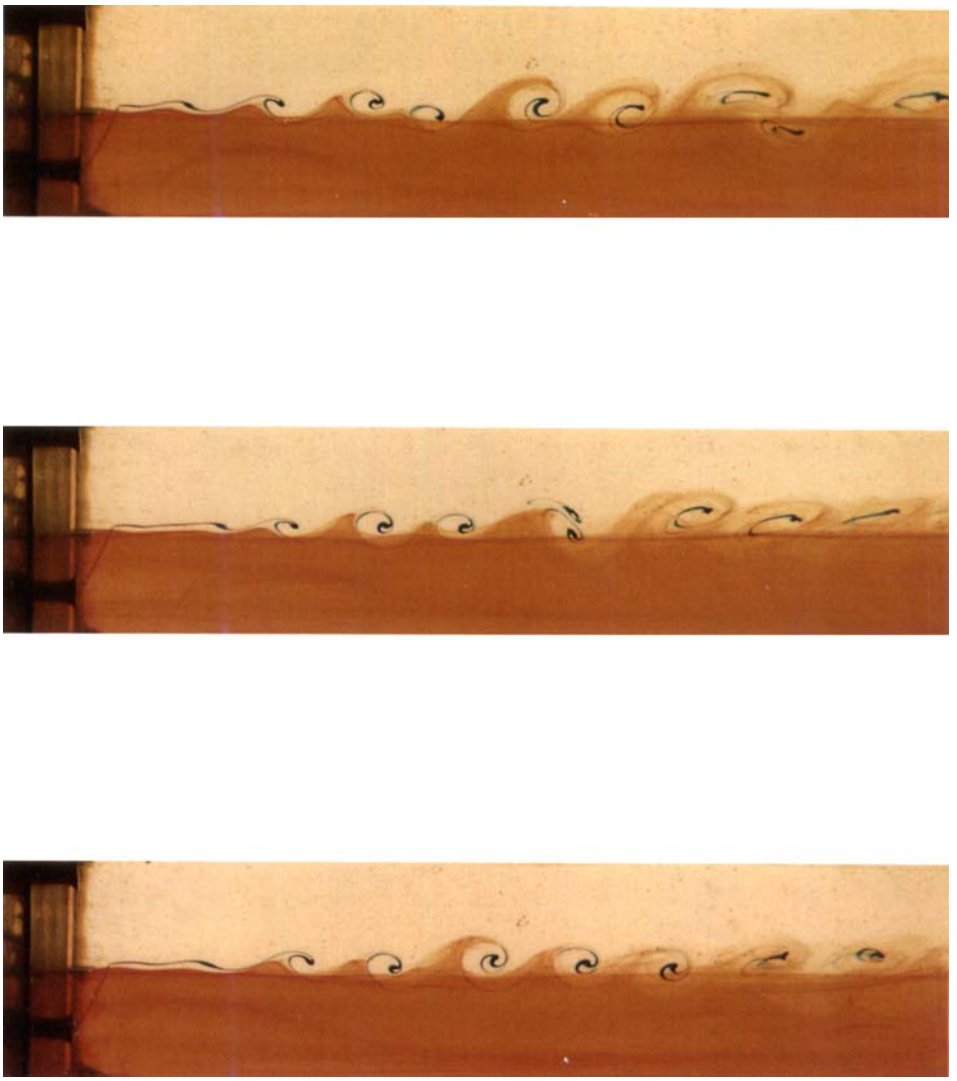

FIGURE 4. Side-view visualization of the two-dimensional base-flow. Both the interface and the position of the core of the spanwise vortex tubes are seen. Note that, owing to the wake component, the spanwise eddies have their axis initially just slightly above the interface. Also observe that since the Kelvin–Helmholtz instability has not been forced, the location of the first vortex pairing is not fixed.

in the shear layer, the vorticity concentrates in vortex tubes which dominate the flow. Under these idealized conditions, the evolution of the interface will mark precisely the process of the concentration of vorticity (at least during the initial stages of the development of the instability when diffusion of the vorticity due to viscous effects can be neglected).

In our experiments, however, because of the finite thickness of both boundary layers emanating from the plate, the vorticity was not initially confined to the interface but rather was distributed over a fairly thick layer (momentum thickness ≈ 2 mm). In this case, when the primary shear instability occurs, the position of the interface will not reveal the precise location and distribution of the vorticity. Nevertheless, as in the ideal case, the deformation of the interface follows qualitatively the evolution of the vorticity. This 'qualitative' correlation between vorticity concentration and interface deformation can still be used to analyse the evolution of the vorticity and thus of the flow instabilities.

To illustrate this important point and the difficulties associated with it, we will analyse the case of the two-dimensional shear layer used as the base-flow in our study. Figure 4 (Plate 1) shows side views of the unperturbed base-flow in which both the interface and the position of the vortex tubes were visualized by additional injections of dye at several heights above the interface. From this side view, it can be seen how, as the two-dimensional instability develops, spanwise vortex tubes form with their axes just slightly above the interface. Notice that while vorticity has already concentrated to reveal the presence of a vortex tube, the interface has not fully rolled up and exhibits only an undulation, (first and second vortices in figure 4). When the vortex tubes convect downstream, then the interface is observed to corrugate quickly and progressively roll up and wrap around them. Although, as was pointed out before, one should be cautious in establishing a 'quantitative' correlation between the evolution of the interface and that of the vorticity, it is clear that if the interface is observed progressively folding in and wrapping around at a given location, it can be said that vorticity must have been concentrating there in an appreciable amount. This is precisely the correlation which we have used in our analysis.

In our experiments we combined several flow-visualization techniques in order to establish the 'qualitative' correlation that exists between the process of concentration of vorticity and that of the evolution of the interface. By visualizing the temporal and spatial evolutions of the interface we tracked down the concentration of vorticity, thus obtaining a 'qualitative' description of its evolutions. From the analysis of this process, we were then able to study the development of the different instabilities which occur in the shear-layer.

3. Response of the two-dimensional base-flow to perturbations periodically placed along the span

We will begin by analysing a representative case corresponding to the plane free shear layer subjected to a single-wave horizontal spanwise disturbance of amplitude $a = 8$ mm and wavelength $\lambda = 4.15$ cm produced by an indented splitter plate of the type shown in figure 2.

A composite flow visualization of this representative case is given in figure 5. The plan view (*a*) shows the evolutions of the interface through the use of the chemical reaction as the Cresol Red responded to changes in the pH (DIV). The splitter plate trailing edge is shown in the far left of this plan view. Two simultaneous cross-cuts,

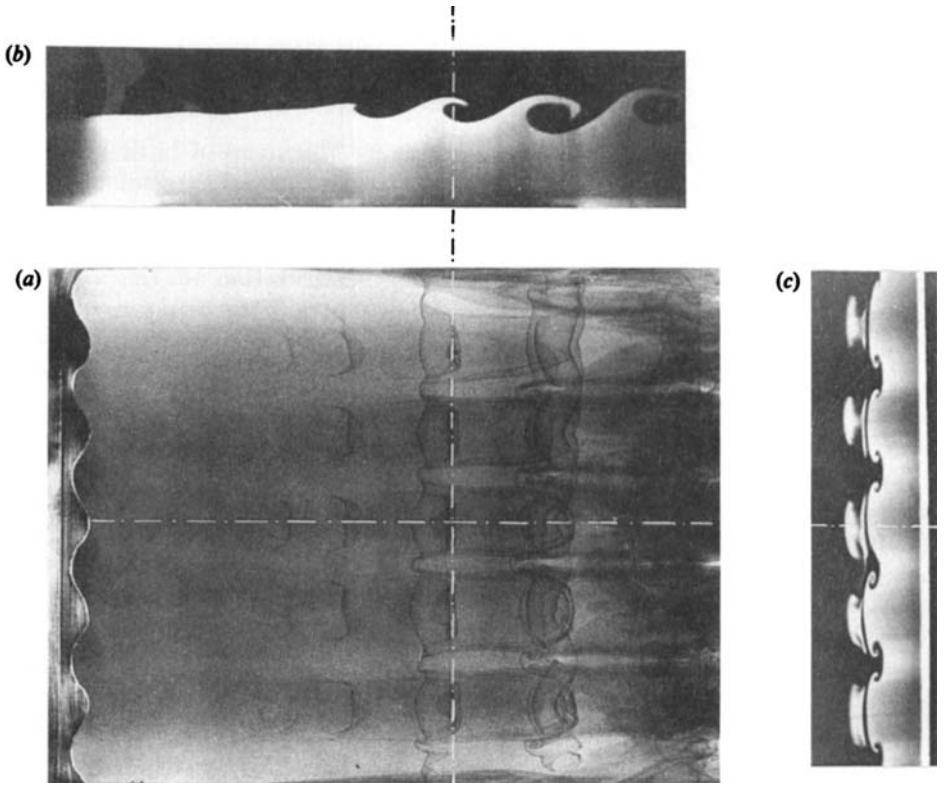

FIGURE 5. Composite flow visualization of the plane shear layer subjected to a single horizontal perturbation of wavelength $\lambda = 4.15$ cm and amplitude $a = 8$ mm. (*a*) Plan view obtained using the DIV technique. (*b*) and (*c*) LIF simultaneous cross-cuts. (*b*) Cross-cut side view of a vertical plane XY through the central axis of the channel. (*c*) Cross-cut end-view of a plane parallel to YZ.

using LIF, are also shown in the figure. Figure 5(*b*) corresponds to the cross-cut side view of a vertical (X, Y)-plane through the central axis of the channel. Figure 5(*c*) shows the vertical cross-cut, end view of a plane parallel to the (Y, Z)-plane. The position of both planes is shown in the plan view by white, dashed lines.

From these combined visualizations, several important features of the flow are readily apparent: (i) the onset of the Kelvin–Helmholtz instability; therefore, the concentration of spanwise vorticity has not been prevented by the effect of the perturbation. Observe from the plan view (figure 5*a*) that although achieving a sinusoidal undulation, the axis of the spanwise vortices remains perpendicular to the flow direction. (ii) In addition to the above described concentration of spanwise vorticity, a well-organized array of streamwise vortices appears superimposed onto the spanwise vortical structure. The axes of these streamwise vortices align along the axial flow direction. (iii) A pair of streamwise vortices of opposite sign have formed for each wavelength in the indentation of the plate. These pairs of streamwise vortices are not aligned with positions corresponding to the inflexion points in the indentations of the splitter plate, nor is their spacing constant across the span. Observed in the plan view (figure 5*a*) that the spacing between the counter-rotating vortices is greater in the positions aligned with the tips of the indented splitter plate while they are closer to each other in positions aligned with the dents of the plate. (iv) The large, spanwise vortices acquire a wavy undulation of the same wavelength

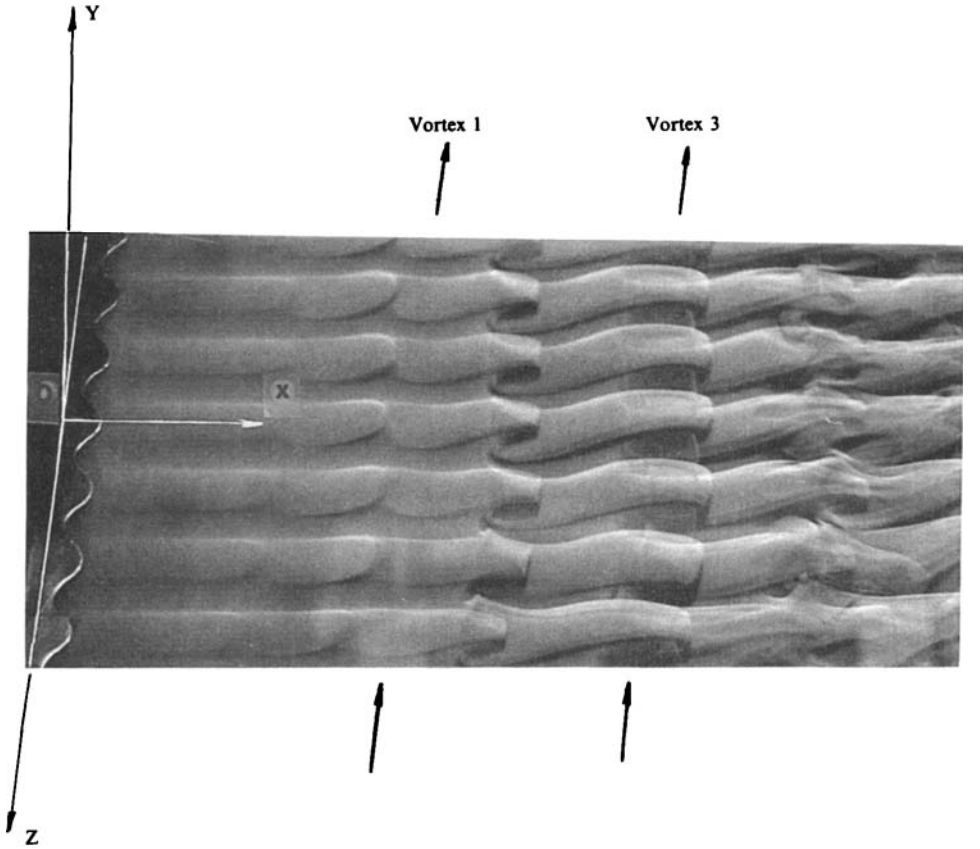

FIGURE 6. Spotlight induced fluorescence perspective view of the interface. The interface is viewed through the transparent upper stream as the fluorescence of the lower stream is excited. Note the full roll-up of the interface already apparent at the position marked as vortex 3.

as the indentations in the splitter plate. However, the undulations of the spanwise vortex tubes are 180° phase shifted with respect to the sinusoidal indentations in the plate.

The above results confirm the observations of Wygnanski *et al.* (1979), Browand & Troutt (1980), Breidenthal (1980), Roshko (1980), Oguchi & Inoue (1984) and others who have shown that even under the influence of strong external disturbances, the mixing layer is eventually dominated by the presence of a quasi-two-dimensional spanwise vortical structure.

With a high concentration of fluorescein particles in the lower stream, the three-dimensional interface separating the two streams was also visualized by inducing the fluorescein of the particles with a spotlight. Using this method, a perspective view of the interface is shown in figure 6. This perspective view reveals the same qualitative features described above; namely, the co-existence of both stream and spanwise vortices. Dye initially injected above the splitter plate (similar to the case shown in figure 4), reveals, as early as at the position marked by vortex 1 in figure 6, the presence of a vortex tube extending all along the span. When these spanwise vortex tubes are convected downstream, the interface progressively wraps around them. Notice in the perspective view how at a position marked by vortex 3 the spanwise

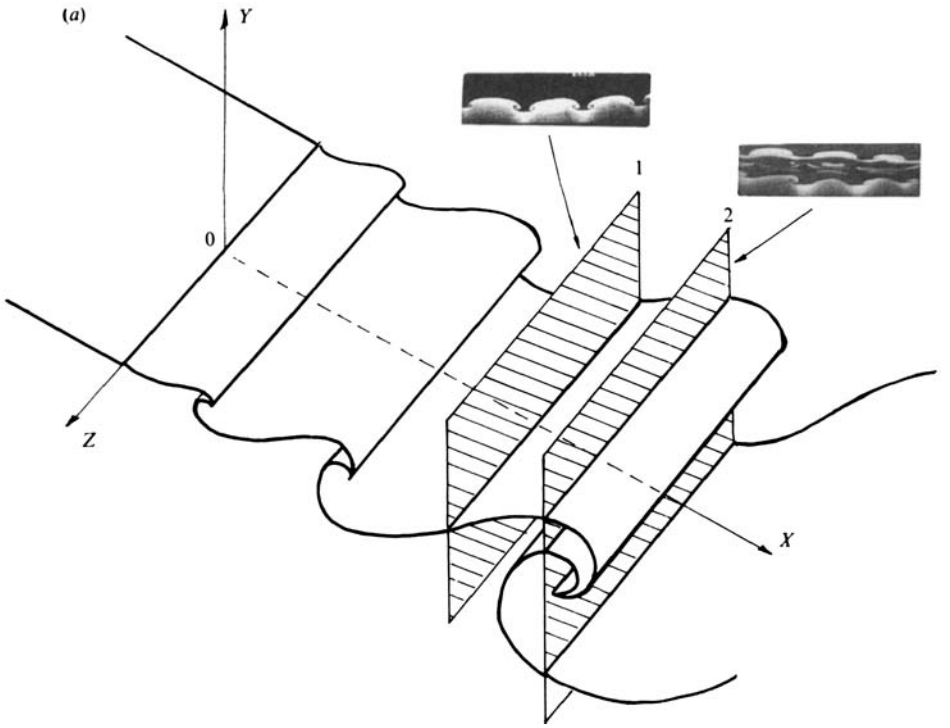

FIGURE 7(a). For caption see facing page.

vortex tube has already caused the full wrapping around of the interface all along the span.

To further analyse the concentration of streamwise vorticity, we followed the evolutions of the interface on the braids between two consecutive spanwise vortices (position indicated by the illuminated plane 1 in figure 7*a*) as they were convected downstream. A plane of laser light parallel to the (Y, Z)-plane (perpendicular to the axial flow direction) was moved downstream along the X-axis, with a velocity equal to the convection velocity of the spanwise structures (approximately 2.4 cm/s). The plane was visualized using LIF of the fluorescein particles added to the lower stream. A near-end view of the plane was taken by placing the camera at a small angle α with respect to the X-axis above the free water surface (figure 7b). The position of the interface was then recorded as the X-coordinate was increased. Figure 8 shows five pictures of the interface at a location corresponding to a braid region at distances of 10.16 cm, 12.70 cm, 15.24 cm, 17.78 cm, and 20.32 cm downstream of the origin of the mixing layer, with the X-coordinate increasing from the top to the bottom of the figure. From this convected evolution of the interface, it can be seen that the interface has progressively folded and wrapped around, acquiring a mushroom-type shape. For this braid location, the unequal spacing between consecutive streamwise vortices of opposite sign is quite apparent. The distance between the vortices composing the pair pushing the upper (fast) fluid into the lower one (L_1) is considerably smaller than that of the vortex pair lifting the lower (slow) fluid into the upper one (L_2).

Because of the change in the index of refraction across the free surface of the water, the recorded pictures of figure 8 are distorted (compressed in the vertical Y-direction)

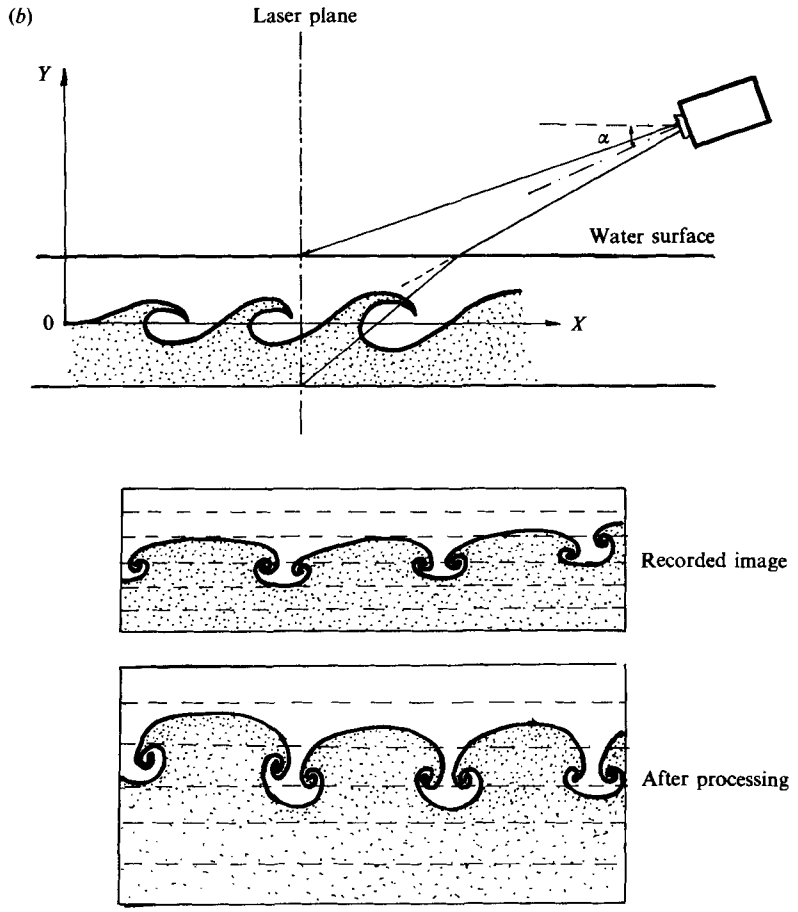

FIGURE 7. (*a*) Perspective view of the interface showing two illuminating laser planes: 1. Through the braid 2. Through the core. (*b*) Cross-cut end-view acquisition method and image restoration. Because of the change in the index of refraction across the interface, the recorded images are compressed in the vertical Y-direction. Each frame is restored to its actual size using digital image processing techniques.

and do not correspond to the actual, geometrical shape (see figure 7). Using image-processing techniques, the recorded images were stretched vertically along horizontal bands to achieve the true shape of the interface. Through the use of the visualization of a calibrated grid placed at the position of the recorded planes, the stretching factors applicable for the different horizontal bands in which the image was discretized were calculated in each case. The recorded images were first digitized and filtered for background noise. Owing to the almost binary nature of the image, a multi-threshold technique was applied to obtain a sharp definition of the edge which determined the interface position. Figure 9(*a*) shows the results of the combined filtering and thresholding operations for planes corresponding to positions $X = 5.08$ cm, 7.62 cm, 10.16 cm, 12.70 cm, 15.24 cm, 17.78 cm, 20.32 cm. When the corresponding stretching (expansion) factors were applied to each of the horizontal bands in which the image was discretized, a geometrical restoration of the interface was obtained. Figure 9(*b*) shows the actual interface shape after image restoration of the seven binary images corresponding to the locations listed above. Notice that the

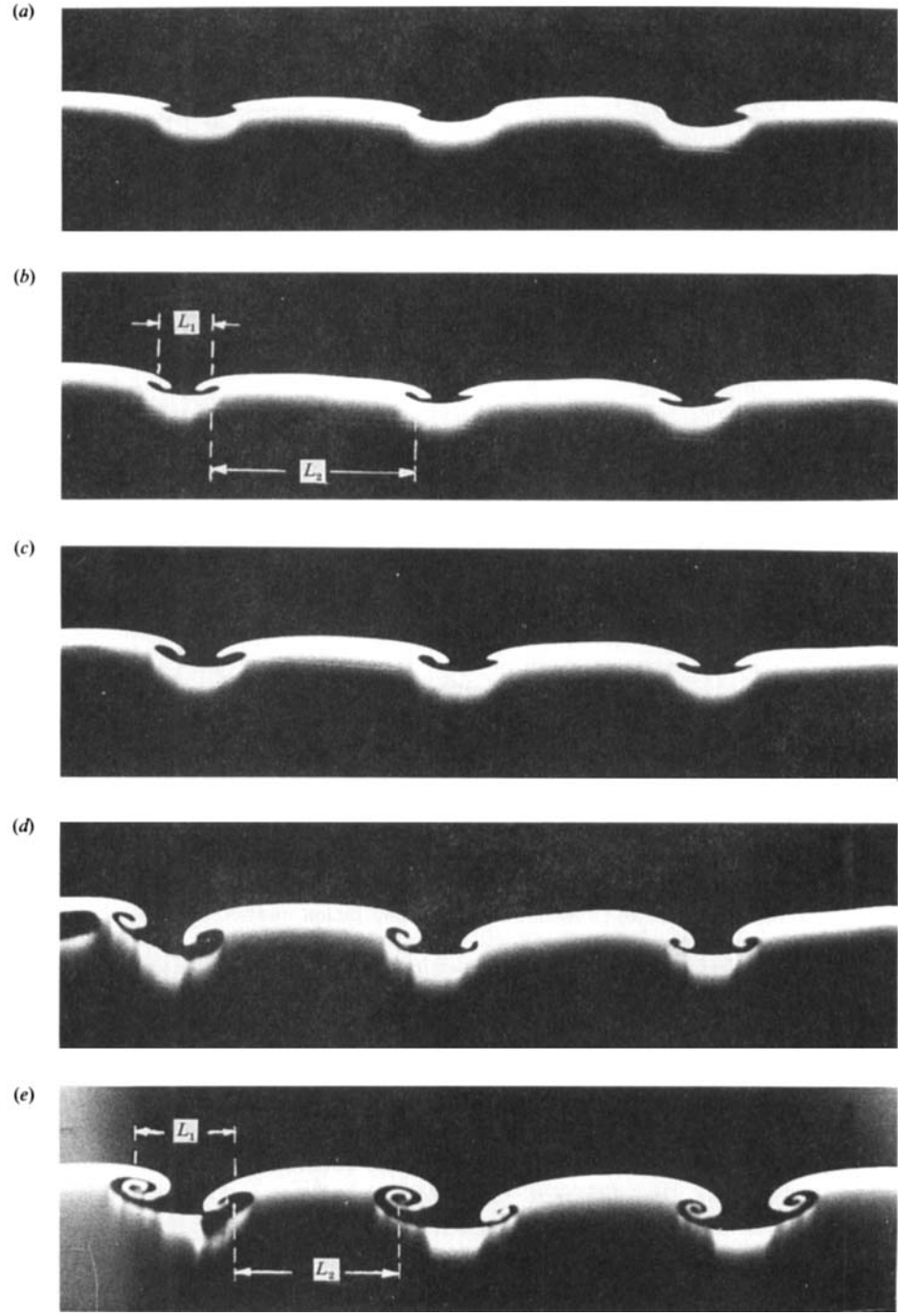

FIGURE 8. LIF end-view cross-cuts of the braid at distances of 10.16 cm, 12.70 cm, 15.24 cm, 17.78 cm and 20.32 cm downstream of the origin of the mixing layer. Distance increasing from the top to bottom of the figure. Note the unequal spacing between the counter-rotating pairs of streamwise vortices. The distance between the vortices of the pair pushing the fast fluid into the lower (slow) one (L_1) is smaller than the distance between the vortices of the pair lifting the slow fluid into the fast (upper) one (L_2). L_1 and L_2 becoming equal as we move downstream.

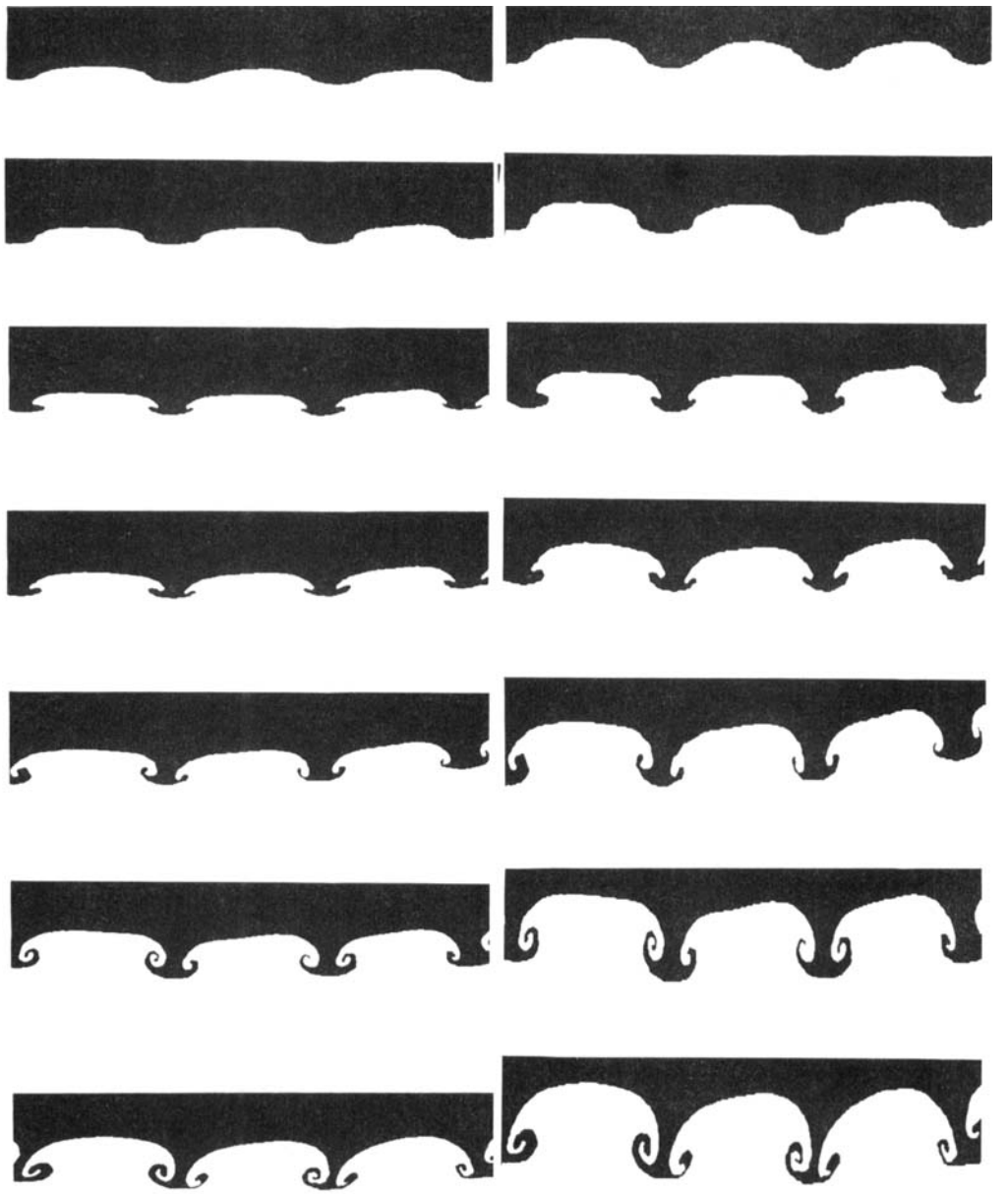

FIGURE 9. (*a*) Digitized end-view cross-cuts images after a Laplacian filter and a threshold have been applied. The binary picture show the interface and the volumes occupied by both streams at positions $X = 5.08$ cm; 7.62 cm; 10.16 cm; 12.70 cm; 15.24 cm; 17.78 cm; and 20.32 cm (X increasing from top to bottom of the figure). (*b*) Actual interface shape after the digital image processing and stretching factors are applied.

interface roll-ups reveal an almost circular shape similar to Lin & Corcos' (1984) calculations.

To study the interaction of the spanwise vortex tubes with the evolving streamwise vortex pairs, video recordings as well as cinematography were used. A sequence of consecutive pictures taken at 10 f.p.s. of a fixed vertical plane (parallel to the (Y, Z)-plane) at a distance downstream of $x = 17.78$ cm is shown in figure 10.

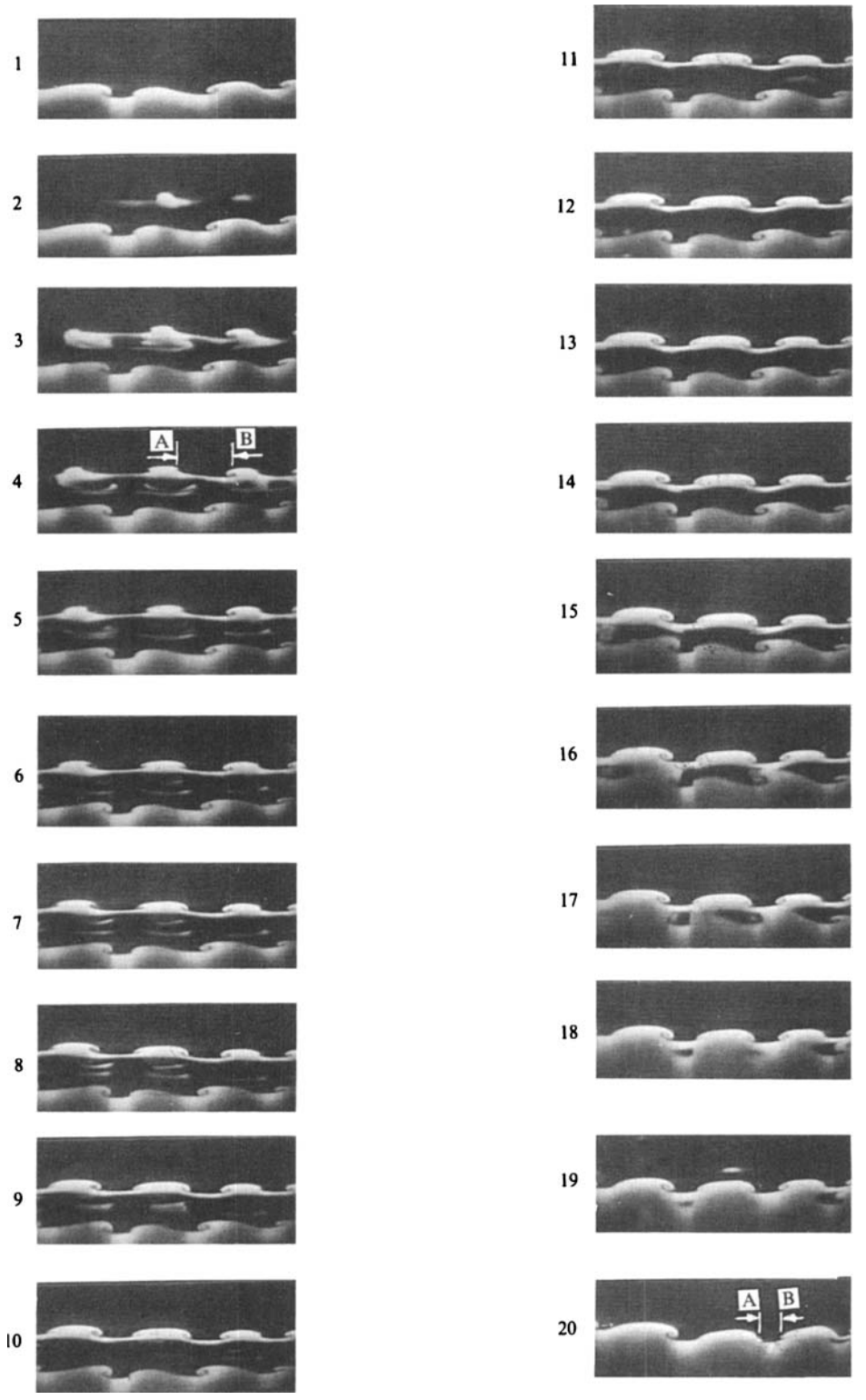

FIGURE 10. For caption see facing page.

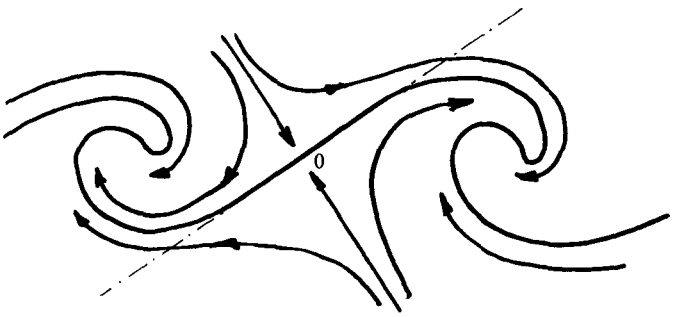

FIGURE 11. Sketch of the structure of the two-dimensional velocity field in the reference frame moving with the average velocity of the spanwise vortices. The position of the free stagnation point (0) as well as the principal direction of positive strain rate is shown.

The consecutive frames show the passage of one spanwise vortex beginning with the braid connecting the vortex to the previous one (frame 1) and ending with a similar view of the braid connecting the vortex to the following one (frame 20). At this downstream location, the spanwise vortex has already caused the full roll-up of the interface (see frames 4–15). The streamwise vortex tubes, under the effect of the spanwise vortices, are observed to wrap around them. As they envelop the spanwise rollers, the two-dimensionality of the spanwise vortex cores is not broken, as inferred by the almost straight tube formed by the interface. Furthermore, these pairs of counter-rotating streamwise vortices do not maintain a constant spanwise spacing. Notice, for example, how the distance between the two counter-rotating vortices A and B changes appreciably between the braid (frame 20) and core locations (frame 4).

4. Mechanism for the three-dimensional instability

We will begin by analysing the case presented thus far where the base-flow is subjected to a single-wave sinusoidal horizontal perturbation of small amplitude. Under the effect of the Kelvin–Helmholtz instability, the vorticity sheet emanating from the plate is redistributed into regions of strong vorticity (the cores of the spanwise vortices) and weak vorticity (the braids connecting consecutive spanwise vortices). As the instability amplifies, the evolving spanwise vortices begin to develop strain fields in the braids connecting them. In a reference frame moving with the average velocity of these spanwise vortices, the strain field develops the qualitative features shown in figure 11. In the topological structure of the vector field represented by the streamlines, we can identify the existence of saddle points (free stagnation points) in the braid regions between spanwise vortices. The perturbation components of the vorticity present near the stagnation region on the braids are thereby subjected to stretching along the principal direction of positive strain. This

FIGURE 10. Sequence of consecutive frames taken at 10 f.p.s. of a fixed, vertical plane (parallel to the (Y, Z)-plane) at a distance of 17.78 cm from the origin of the mixing layer showing the passage of one spanwise vortex. Frame 1 corresponds to the braid connecting the vortex to the upstream one and frame 20 corresponds to the braid connecting the vortex to the following one downstream. Observe that the spacing between two counter-rotating vortices A and B do not remain constant. The distance between them increasing as we move into the core.

stretching is the mechanism responsible for the concentration of axial vorticity that results in the formation of the streamwise vortex tubes.

Let 1 and 2 (figure 12) represent two consecutive spanwise vortices formed through the two-dimensional, Kelvin–Helmholtz instability. The vorticity that still exists on the braids is represented in the figure by line vortices that, for simplicity, are indicated by one vortex filament situated in the stagnation region between the two consecutive spanwise vortices. These vortex lines as well as the spanwise vortex tubes contain the imposed, single-wave perturbation of small amplitude (not shown in the figure). As the vorticity continues concentrating in the cores of the spanwise vortices, the perturbed vorticity of the braids is subjected to an increasingly stronger strain field. The vortex filaments on the braids then experience a progressive stretching along the direction of the principal plane of positive strain, evolving into counter-rotating pairs of vortex loops shown schematically in figure 12(*a–c*). The maximum amplification occurs with the vortex lines lying near the free stagnation point where the positive strain is maximum. As the amplification process continues through stretching, the evolving axial loops envelop the large spanwise vortex tubes (figure 12*d*). At this point, the topology of the vorticity field is similar to the one suggested by Bernal (1981) and further inferred by Jimenez *et al.* (1985) through the three-dimensional digital image processing of Bernal's flow visualizations.

The experimentally observed evolution of three-dimensional instability described above supports the hypothesis postulated by Corcos and co-authors and used in their analysis of the origin of the three-dimensional motion (Corcos & Lin 1984; Lin & Corcos 1984) i.e. the development of the two-dimensional instability (the strain field) is essential to the formation of the streamwise vortex tubes. Corcos (1979), Corcos & Lin (1984) and Lin & Corcos (1984) studied the evolution of an array of alternating sign, weak vortices with axes parallel to the direction of a uniform positive strain field. Their numerical results show that the weak streamwise vorticity may evolve into concentrated, round vortices for certain values of the strain rate and distance between axial vortices.

The same qualitative development observed in our experiments has also been found through the analysis of a perturbed plane free shear layer via three-dimensional inviscid vortex dynamics. Using this approach, Ashurst & Meiburg (1988) analysed the development of three-dimensionality in a plane free shear layer subjected to a single-wave perturbation in the initial conditions. Their temporally developing shear layer, whose vorticity was discretized into an array of vortex filaments, shows precisely the sequence of events we observed experientally. Their calculations, which included the two signs of vorticity initially present in our finite boundary-layer-thickness shear layer, show that the characteristic time of the primary Kelvin–Helmholtz instability is much shorter than that of the three-dimensional instability. Thus, once the vorticity has concentrated in an appreciable amount on the spanwise vortex tubes, their results show that under evolving strain fields developed by them, the amplitude of the wavy vortex filaments on the braids grows quickly. As reinforced by our experiments, their results for the case of a very small amplitude of the perturbation show that the instability of the braids occurs initially in an almost uncoupled fashion with the spanwise vortex tubes retaining their two-dimensionality. Although they show that the inclusion of two signs of vorticity (to model the wake component) leads to a more nonlinear development of the three-dimensional structure, calculations performed with only one sign of vorticity (ideal case with no wake component) also reveal the same qualitative evolution of the different instabilities discussed above. The only remarkable

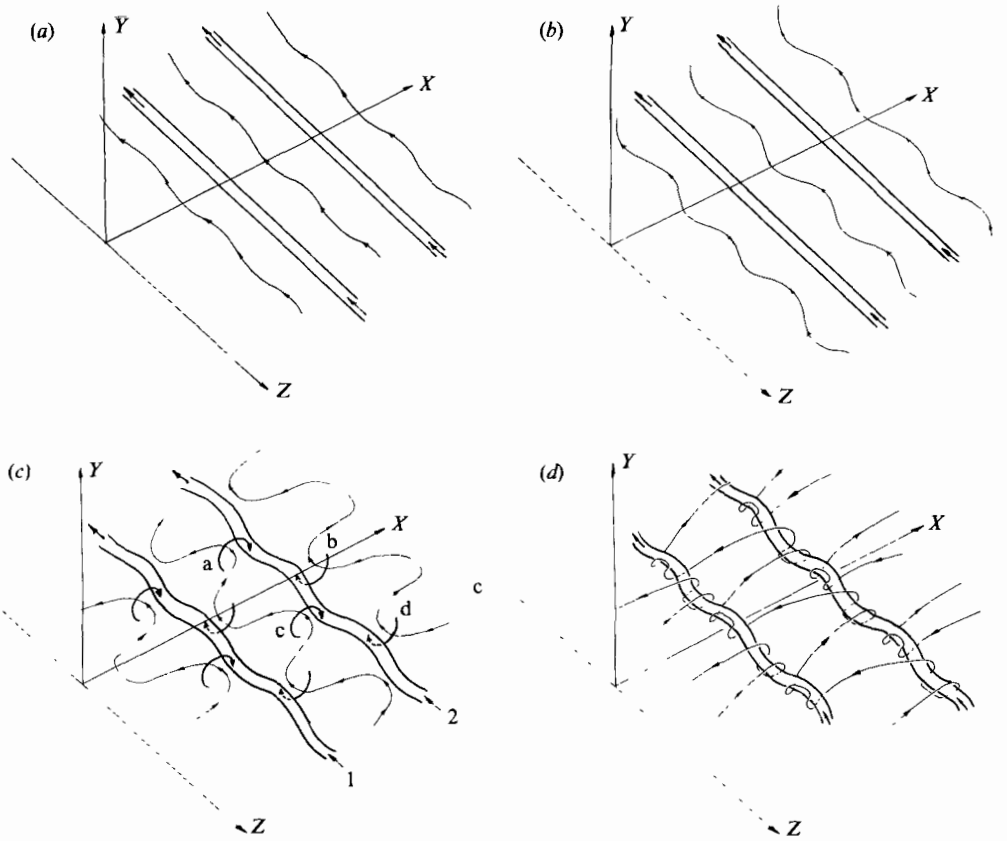

FIGURE 12. Schematic representation of the development of the three-dimensional instability. The perturbation component of the vorticity existing in the braids is amplified through stretching. The maximum amplification occurs along the principal direction of the positive strain at the free stagnation point.

difference between their one-sign- and two-signs-of-vorticity calculations is that in the former the streamwise vortex tubes in the braids form equally spaced, while in the latter they acquire a non-uniform spacing.

The above numerical results suggest that the non-uniform spacing between streamwise vortex tubes observed in our experiments was caused by the interaction between the stronger (upper) and weaker (lower) vorticity emanating from the plate. This 'wake' effect appears to play an important role in the initial orientation and the spacing of the streamwise vortex tubes. Note in figure 8 that near the origin of the mixing layer ($X = 5.08$ cm), where the wake effect is still quite strong, the spacing between the streamwise vortices in the upper stream (L_1) is much greater than in the lower stream (L_2). As one moves downstream ($X = 20.32$ cm), the wake effect disappears and the distances L_1 and L_2 become almost equal.

This complex interaction between the two layers of vorticity, which results not only in above mentioned unequal spacing, but also, in some cases, in the non-axial orientation of the evolving streamwise vortex tubes, has recently been studied both numerically and experimentally by Meiburg & Lasheras (1988). Using three-dimensional vortex dynamics methods and flow-visualization techniques similar to the ones described here, they studied the three-dimensional development of a plane

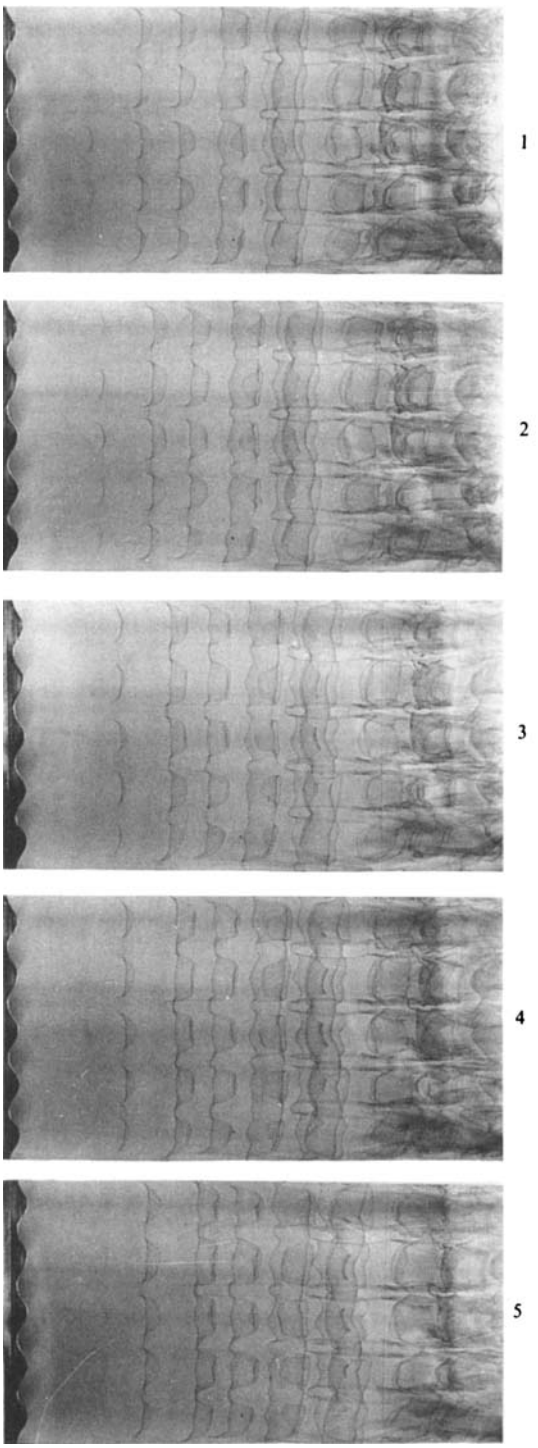

FIGURE 13. Plan views of the temporal evolution of the layer during one second (framing rate 5 f.p.s.), single-wave horizontal-perturbation case. Note the progressive deformation of the spanwise vortex tubes in acquiring a wavy undulation of the same wavelength as the perturbation (indentation in the plate) but 180° phase shifted.

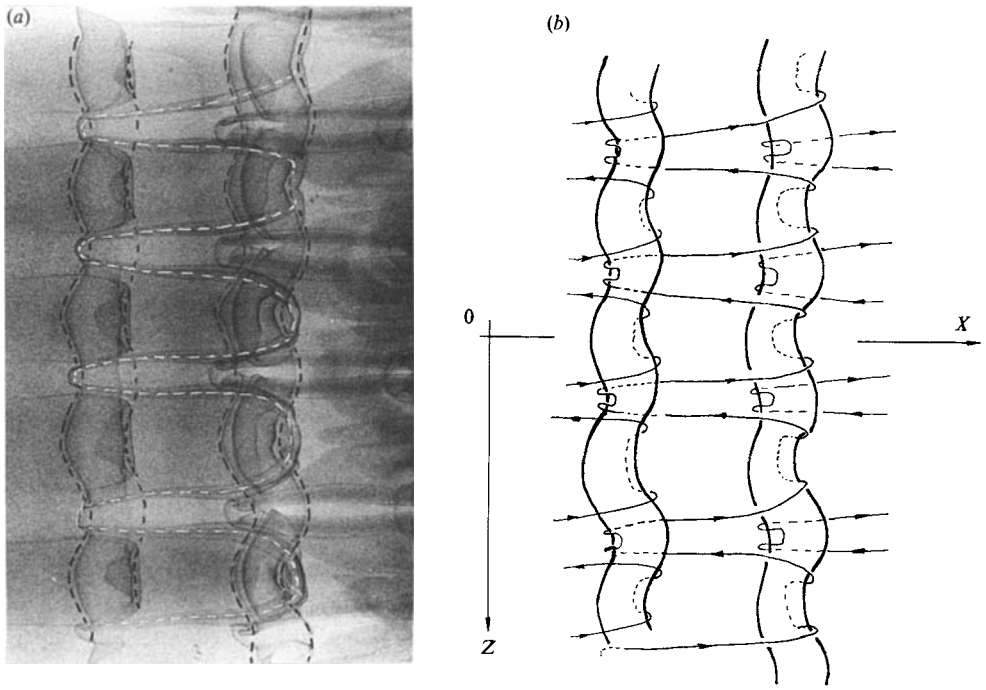

FIGURE 14. Structure of the vorticity field after the axial vortex loops wrap around the spanwise vortices. (*a*) Plan view of the direct interface visualization. (*b*) Topology of the vorticity field between two consecutive spanwise vortices.

wake behind a flat plate. In this limiting case, where the two vorticity sheets of opposite sign emanating from the plate are of the same strength, they show that the interaction between the two layers of opposite sign vorticity caused the streamwise vortex tubes to acquire not only a non-uniform spacing, but also to evolve into λ-shaped structures.

As the amplitude of the wavy perturbations of the filaments amplify, the streamwise vortex tubes formed in the braids begin to interact with the spanwise vortex tubes by wrapping around them. This effect can be observed in the sequence of plane views of the shear layer in figure 13. It shows, from top to bottom, the temporal evolution of the layer during one second (framing rate = 5 f.p.s.). Note the progressive deformation of the spanwise vortex tubes in acquiring a wavy undulation of the same wavelength, but 180° phase shifted with respect to the initial perturbation.

The mechanism for this nonlinear interaction effect leading to the progressive deformation of the spanwise vortex tubes is schematically shown in figure 12(*c*). Let a, b, c, and d represent portions of the hairpin vortices on the braids between the spanwise vortices 1 and 2 and 2 and 3, which have evolved through the convective stretching. Under the effect of the loops a and c, the axis of the vortex tube 2 is lowered into the slow stream, while under the effect of b and d it is lifted into the fast stream. Because of the vertical shear, the portion of vortex 2 under the influence of the hairpin vortices a and c is retarded, while the portion under the effect of b and d is advanced. The final combined effect of the interaction of the streamwise vortex loops with the spanwise vortices is to produce in the latter an undulation of the same wavelength, but 180° phase shifted with respect to the initial perturbation.

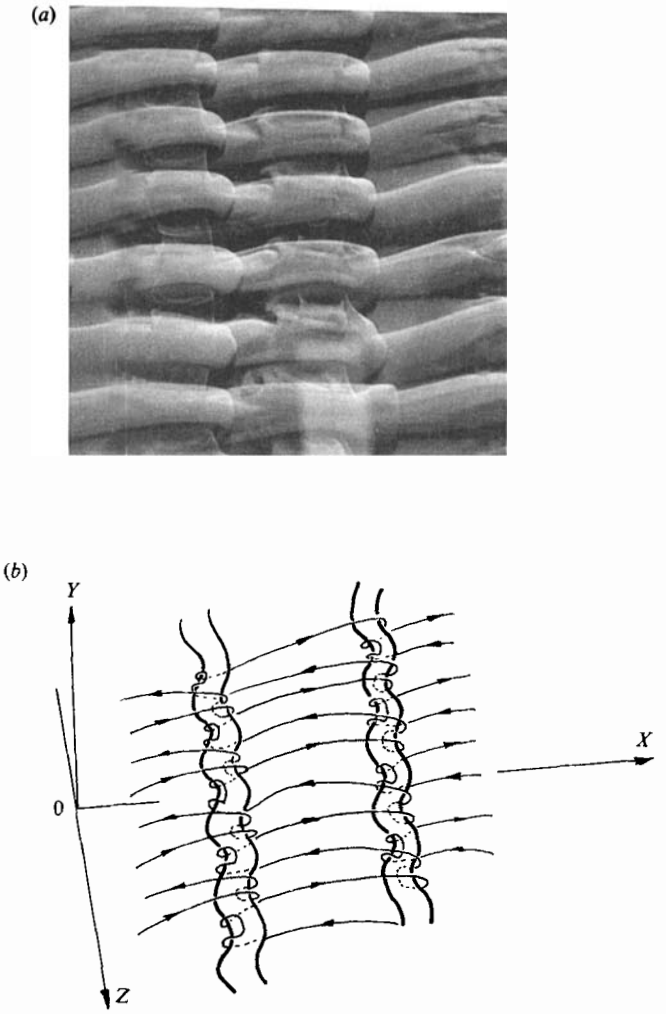

FIGURE 15. Perspective near-side view of the interface (same region as shown in figure 14) using spotlight induced fluorescence.

The resulting structure of the vorticity field achieved at this stage is shown in figures 14, 15 and 16. The plan view in figure 14 shows the organization of the vorticity field existing between two consecutive spanwise vortices. It is apparent in this flow visualization that, while the streamwise vortex tubes in the braids are parallel to each other and oriented along the axial X-direction, they acquire a λ-shape as they envelop the spanwise vortex tubes. Their axes are displaced laterally, becoming almost perpendicular to the wavy cores of the spanwise vortices. Observe in the near-side perspective view of the interface corresponding to this same region (figure 15) that the array of streamwise vortex tubes are lying on a plane inclined to the horizontal (X, Y)-plane (the principal plane of positive strain created by the spanwise vortices). Note also in the near-end perspective view of the interface of figure 16 that six to seven spanwise wavelengths downstream from the origin of the mixing layer, the spanwise rollers already exhibit a wavy undulation on their cores and the streamwise vortex tubes have acquired an almost equal spanwise spacing.

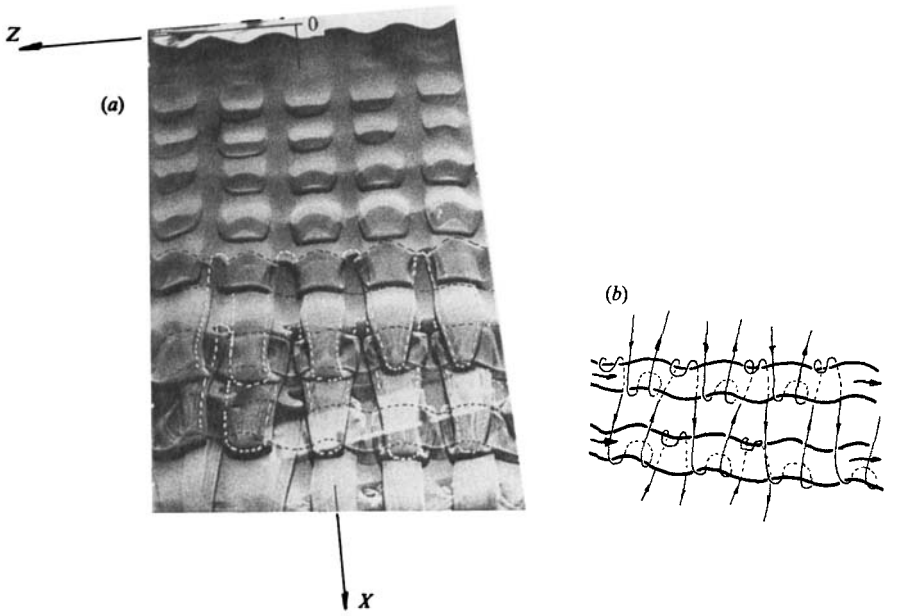

FIGURE 16. Perspective near-end view of the interface using spotlight induced fluorescence.

The inviscid vortex dynamics calculations of Ashurst & Meiburg reveal qualitatively the same experimentally observed, nonlinear interaction process leading to the formation of a wavy undulation of the cores of the spanwise vortices. Their calculations (for both the case of two signs of vorticity and of only one sign) show that the final undulation of the spanwise vortex tubes is of a wavelength equal to that of the initial perturbation, but the phase is shifted 180°.

The growth rate of the amplitude of this wavy undulation in the core of the spanwise vortices was observed to slow down very quickly after a short initial growth period. This initial growth could be related to the linear translative instability of Pierrehumbert & Widnall (1982). However, their mechanism for the formation of the streamwise vortex tubes does not appear to be the one responsible for the concentration of axial vorticity observed in our experiments. Our experimental evidence as well as Ashurst & Meiburg's numerical simulations indicate that the wavy undulation on the cores of the spanwise vortices is caused by the streamwise vortex tubes previously formed in the braids. Thus, the streamwise vortices do not seem to evolve from the translative instability of the cores of the spanwise vortices as could be interpreted from Pierrehumbert & Widnall's linear stability analysis.

After analysing the development of the three-dimensional instability, it has become apparent that the orientation of the axis of the vortex tubes resulting from it is that of the direction of the maximum positive strain rate. Generally, as the spanwise vortices are almost two-dimensional, this maximum positive strain occurs along the axial or streamwise direction. Because of this, we have named this vorticity 'streamwise vorticity' or 'axial vorticity'. However, a much more precise terminology would have been 'strain-oriented vortex tubes'. Later, we will discuss the effect of the strain field in the orientation of these vortex tubes.

5. Effect of the initial conditions

5.1. *Effect of the orientation of the initial perturbation*

The topology of the vorticity field resulting from a single-wave horizontal perturbation (indented splitter plate; figure 17), as well as its temporal and spatial evolution, has already been discussed in §§3 and 4. In the following, we will describe the evolution of the shear layer under the effect of a single-wave vertical perturbation and under the effect of a perturbation with both horizontal and vertical components.

5.1.1. *Single-wave vertical perturbations (corrugated splitter plate)*

Experiments conducted with the perturbation resulting from the use of the corrugated splitter plate show essentially the same three-dimensional development of the plane shear layer observed for the case of the horizontal perturbation. Figure 18 shows the plan view of the plane free shear layer subjected to a single-wave sinusoidal vertical perturbation resulting from a corrugated splitter plate containing an undulation of amplitude $a = 3$ mm and wavelength $\lambda = 3.5$ cm. As was the case with the horizontal perturbation, for each wavelength in the corrugation of the plate, a pair of counter-rotating streamwise vortex tubes form. The spanwise spacing between these streamwise vortex tubes is smaller in positions aligned with the valleys of the corrugation, while it is large in the positions aligned with the peaks.

It is evident from a comparison between these results (figure 18) and the ones obtained with the indented splitter plate (figure 17) that both types of perturbation result in similar three-dimensional structures. The similarities existing between these two types of perturbation result from the effect of the vertical shear on the perturbed vortex lines. A wavy undulation in the vertical (Y, Z)-plane of a vortex filament in the braids is tilted under the vertical shear into the direction of the principal plane of positive strain rate as the upper (faster) stream advances, and the lower (slower) stream retards the respective loops as shown in figure 19. Consequently, after its initial development, the plane free shear layer subjected to the vertical single-wave perturbation resulting from the corrugation, duplicates the flow configuration which develops from a horizontal single-wave perturbation of the same wavelength. The peaks of the corrugations corresponds to the tips of the indentations while the valleys correspond to the dents.

5.1.2. *Combined horizontal and vertical perturbation (indented, corrugated splitter plate)*

When a vertical perturbation of the same wavelength was superimposed 'in phase' with a horizontal one (corrugating the indented plate with the peaks of the corrugation 'in phase' with the tips of the indentation), the shear layer developed the three-dimensional structure observed for the case of a single-wave horizontal perturbation. However, when the vertical perturbation component was 180° phase shifted with respect to the horizontal perturbation (the valleys of the corrugations in phase with the tips of the indentations), it was found that the vertical component suppressed and even in some cases reversed the effect of the horizontal component.

To document this latter effect, we studied the '180° out-of-phase' combined-perturbation case where for a fixed wavelength ($\lambda = 4.15$ cm), the amplitude of the indentation was always kept constant ($a = 8$ mm), while the amplitude of the corrugation was systematically increased from 0 to 6 mm in increments of 1 mm. For the case where the amplitude of the corrugation was very small, < 2 mm), the flow configuration developed was essentially similar to the single-wave horizontal

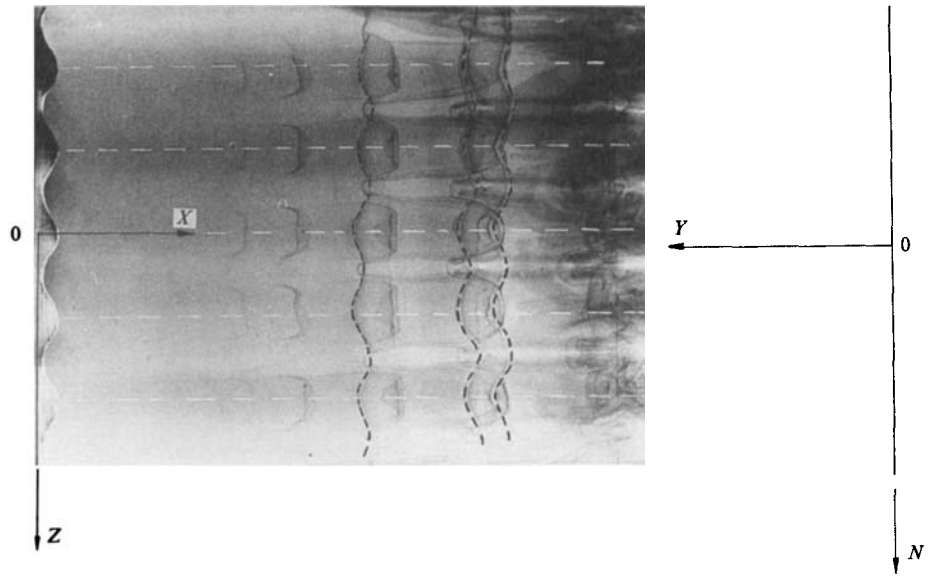

FIGURE 17. Plan view of the indented flat splitter plate case. ($\lambda = 4.15$ cm, $a = 8$ mm.)

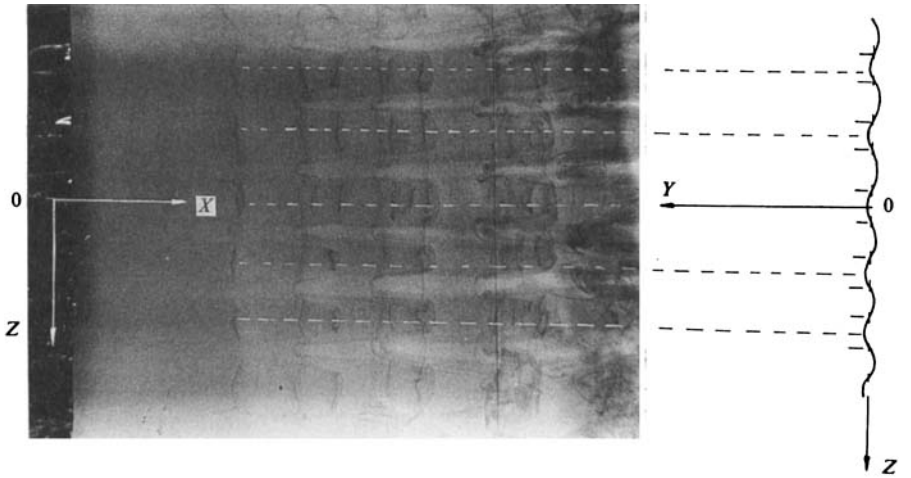

FIGURE 18. Plan view of the corrugated splitter plate case. ($\lambda = 3.5$ cm, $a = 3$ mm.) (Positions aligned with the peaks of the corrugations are indicated in the plan view by white dashed lines.)

perturbation case. As the amplitude was increased (3 mm), a case was achieved where the vertical effect almost cancelled the horizontal perturbation (the vertical component tilted into the horizontal plane resulting in an almost cancellation of the horizontal component). Under these conditions, the flow was observed developing in an almost two-dimensional fashion (figure 20). Notice in figure 20 that the formation of axial vortices, although not fully suppressed, has been retarded. Finally, when the amplitude of the corrugations was further increased (large than 3 mm), the vertical perturbation not only suppressed the horizontal component, but reversed its effect. The three-dimensional flow field achieved in this latter case is shown in figure 21. Notice that in this case, the spanwise vortex tubes have acquired an undulation of

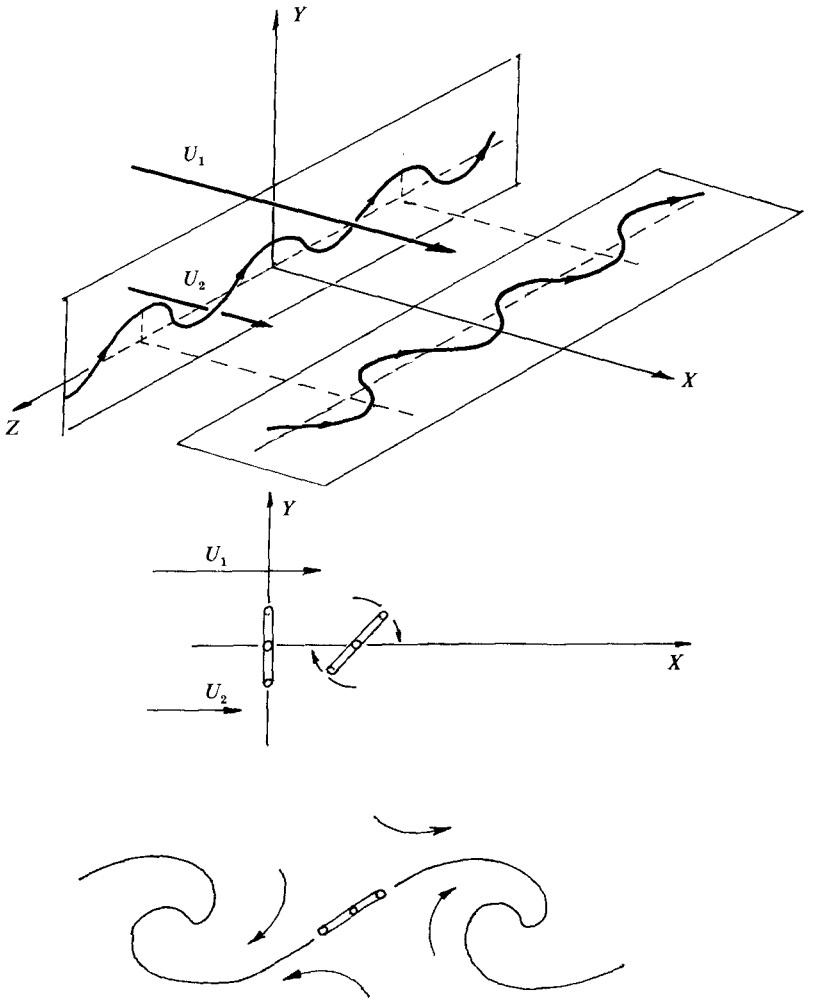

FIGURE 19. A single-wave vertical perturbation is under the effect of the global induction (vertical shear) reoriented (tilted) into the direction of the principal plane of positive strain.

the same wavelength as the perturbation, but now they are 'in phase' with the horizontal perturbation component (indentations in the plate). Also note that the streamwise vortex tubes are more closely spaced in positions aligned with the dents than in positions aligned with the peaks of the corrugated plate (just the opposite of the spacing achieved in the case of the single-wave horizontal component perturbation shown in figure 17).

In summary, depending on the relative magnitude of each perturbation component, the plane shear layer achieves either a topology of the vorticity field where the wavy undulation of the spanwise vortex tubes are in phase or one where they are 180° out of phase with respect to the horizontal perturbation wave. Moreover, the vorticity field (to a first approximation) resulting from a combined perturbation can be described as a linear superposition of the effect of each perturbation component.

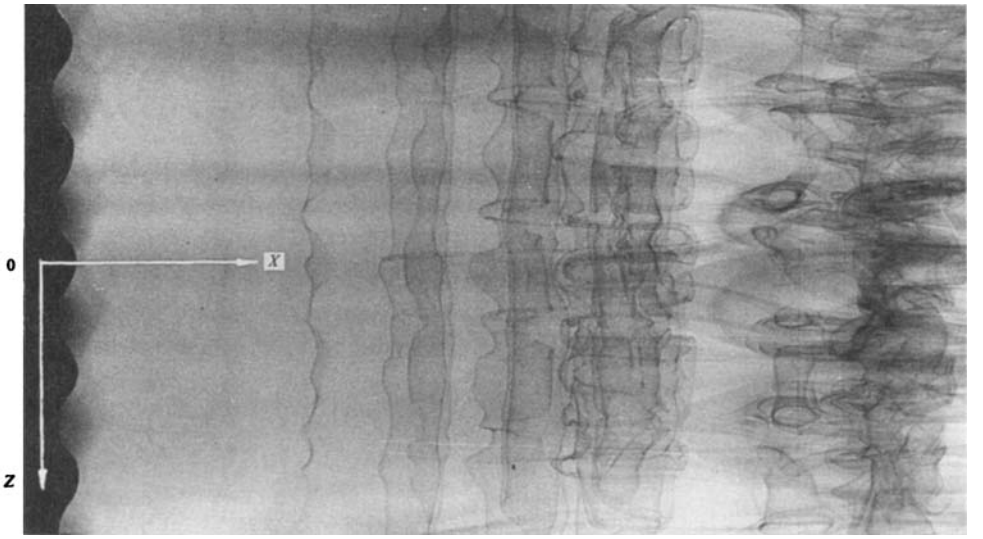

FIGURE 20. Plane view of the '180° out of phase' corrugated, indented splitter plate showing the '*almost*' cancellation of the effect produced by the horizontal component of the perturbation by the vertical one.

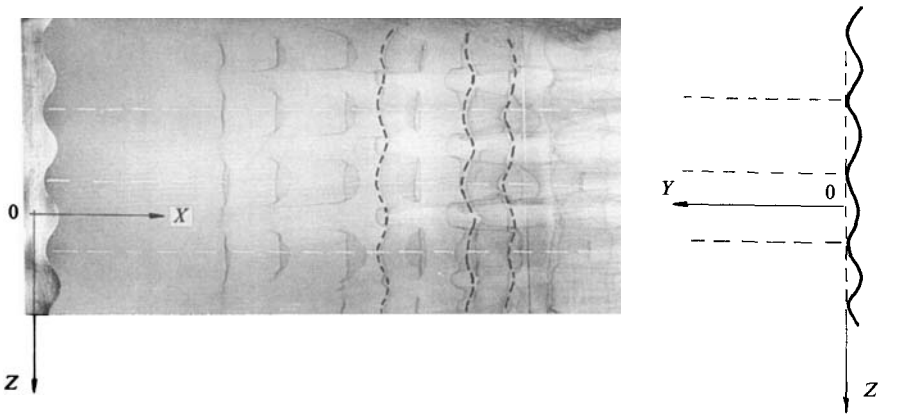

FIGURE 21. Plan view of the layer developing from a perturbation containing both horizontal and vertical components (corrugated indented splitter plate case). A '180° out-of-phase' case. The vertical component has reversed the effect of the horizontal component.

5.2. *Effect of the wavelength of the perturbation*

To analyse the effect of the wavelength of the perturbation and to investigate the possible existence of a most unstable value, the wavelength was systematically varied while the small amplitude of the perturbation was kept constant. As the wavelength of the perturbation was changed, we found that the primary two-dimensional Kelvin–Helmholtz instability was not substantially modified. Thus, the strain field which developed in the braids was always of the same approximate strength. However, since the two-dimensional shear instability was not forced and the flow was left to develop naturally, the frequency of the spanwise vortices exhibited a fairly wide spectrum. Because of this wide spectrum, the base-flow did

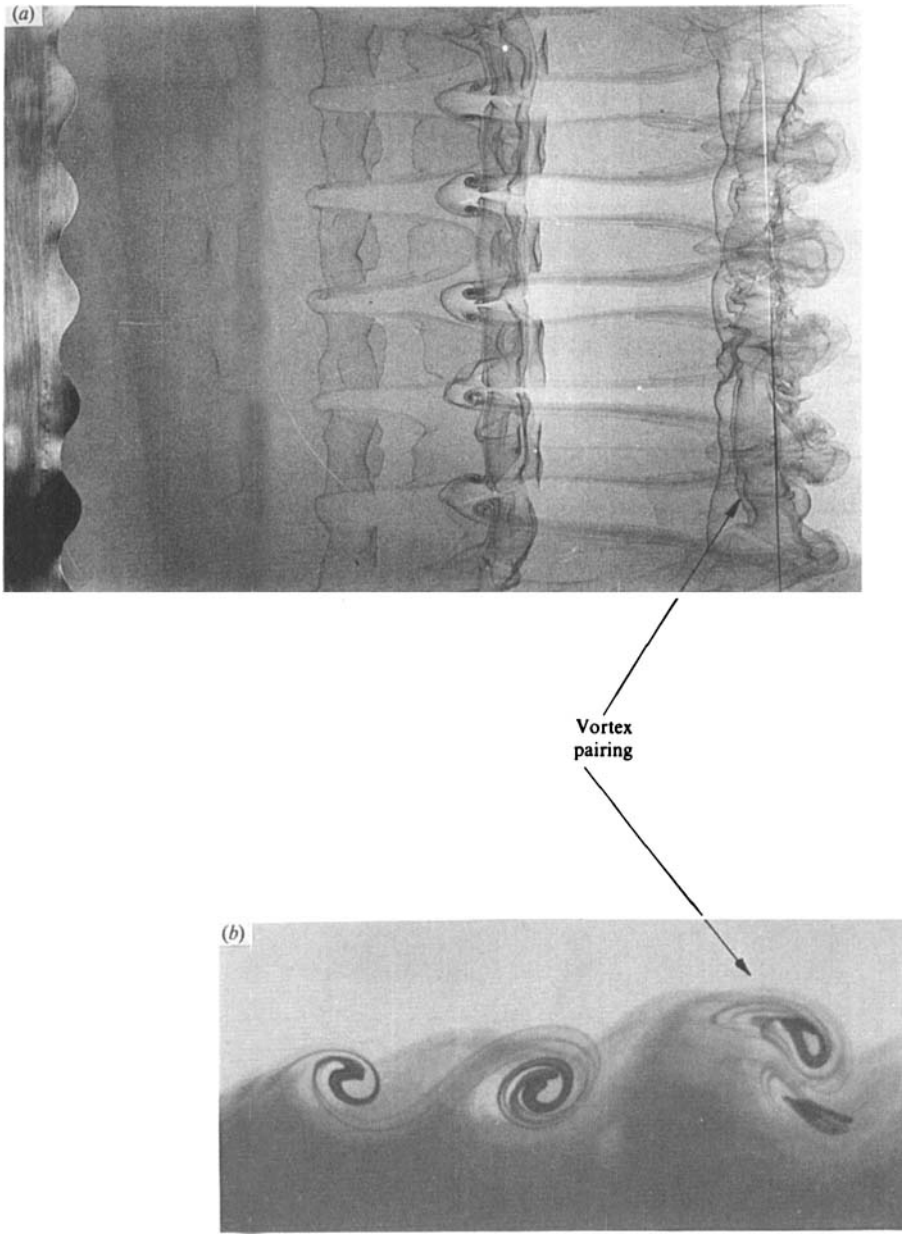

FIGURE 22. Effect of the spanwise vortex pairing on the concentration of axial vorticity. Note that as the vortex pairing occurs, the circulation doubles and initially the positive strain field existing in the braids magnifies, causing an increase in the stretching of the axial vorticity.

not show constant repeatable features to allow a fair comparison of the growth rate of each wavelength perturbation case. In addition, subharmonic instabilities, such as pairing, drastically modified the magnitude of the strain field between consecutive vortices, thus affecting the growth rate of the three-dimensional instability. Figure 22 shows the effect of the pairing between two spanwise vortices on the streamwise vortex tubes. Figure 22 (*a*) corresponds to the top view, while figure 22 (*b*) shows the corresponding side view. As the two consecutive spanwise vortices pair, the

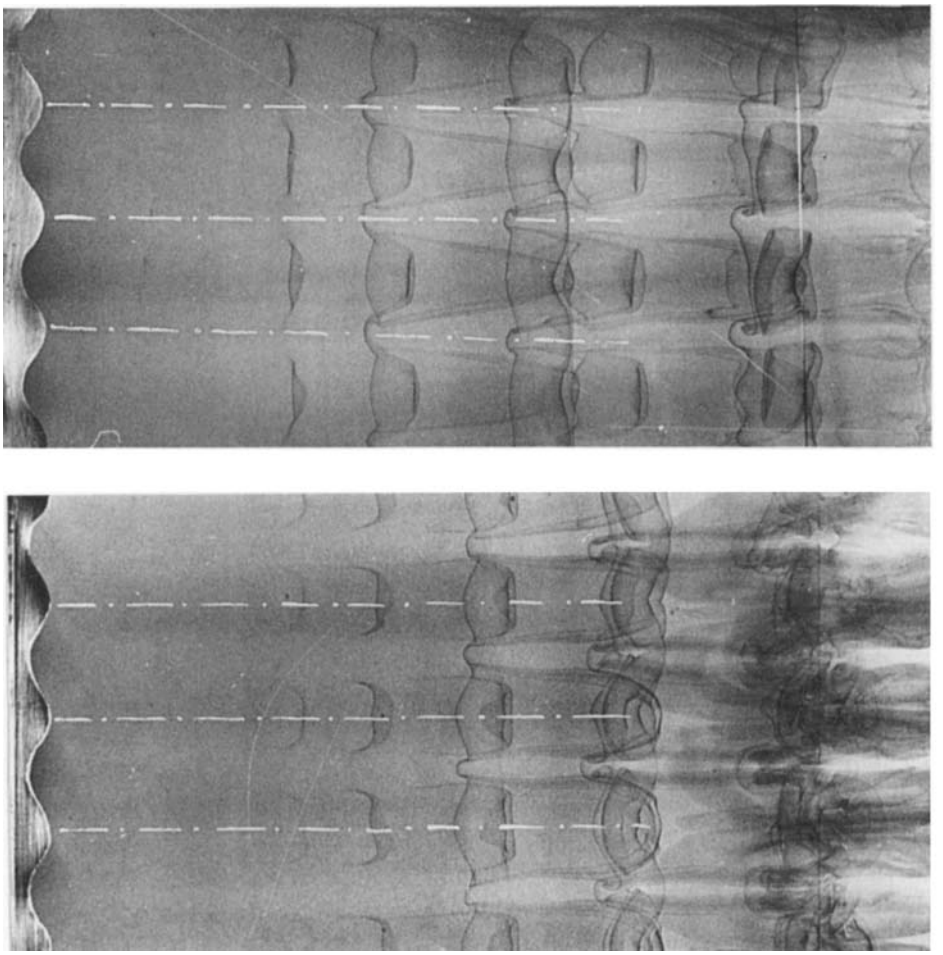

FIGURE 23. Wavelength of the perturbation $\lambda = 4.15$ cm. Corrugated indented splitter plate. (*a*) '180° out-of-phase' case; (*b*) 'in-phase' case.

circulation doubles and we infer that the strain rate on the connecting braids is initially increased. The increased magnitude of the stretching results in a stronger concentration of axial vorticity. Note in the plan view (figure 22*a*) how the diameter of the axial vortex tubes decreases indicating stronger concentrations of vorticity.

Because of the lack of repeatability in the features of the base-flow, we were unable to determine uniquely the existence of a most unstable wavelength. To investigate its existence, the two-dimensional shear instability needs to be forced. In this way, the position and the frequency of the spanwise vortices would be fixed, and a repeatable constant strain field produced. For each case, then, the growth rate of the perturbations could be studied under the same positive strain rate conditions. We are currently conducting this investigation. Although still inconclusive, we have found no appreciable difference in the growth rate for perturbations of wavelengths in the range between $\frac{1}{5}$ and 3 times the Kelvin–Helmholtz wavelength. This suggests that the instability has a large bandwidth of wavelengths for which the growth rate is comparable.

The above discussed effect of the orientation of the initial perturbations (§§5.1.1

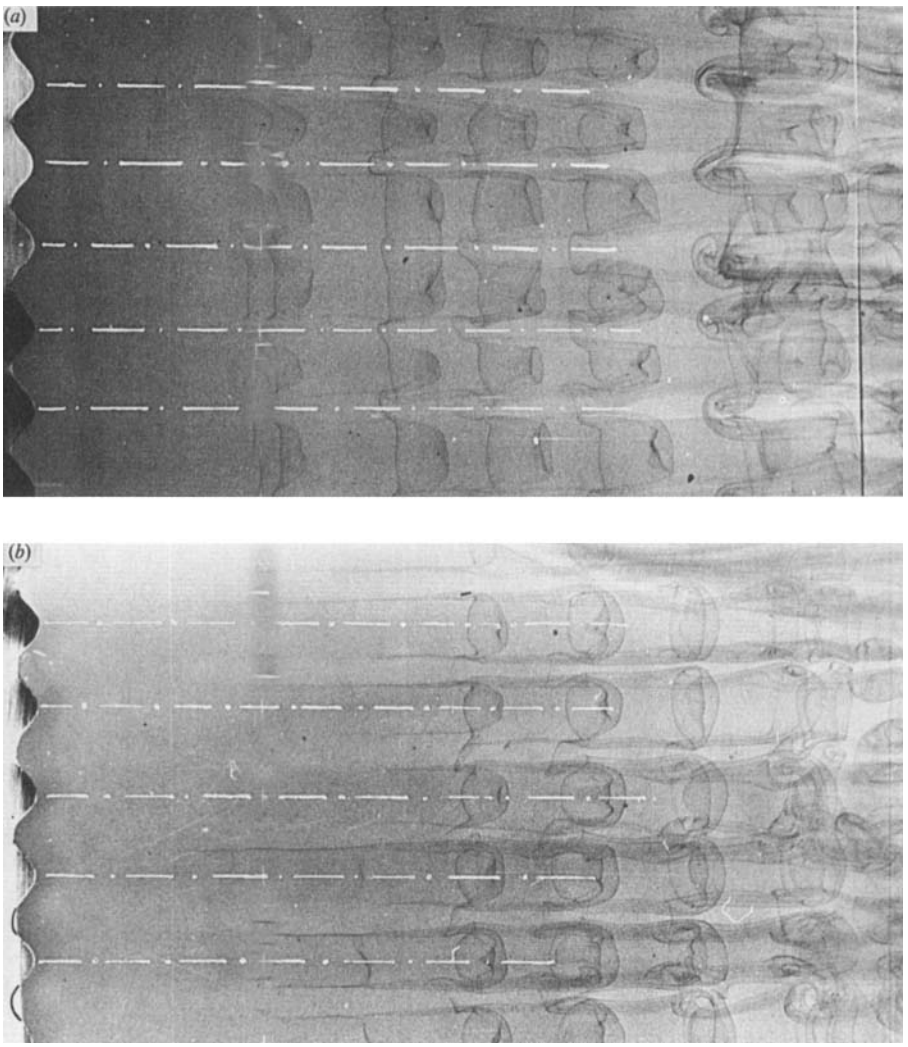

FIGURE 24. Wavelength of the perturbation $\lambda = 3.5$ cm. Corrugated indented splitter plate. (*a*) '180° out-of phase' case, (*b*) 'in-phase' case.

and 5.1.2) was found to be qualitatively independent of the wavelength of the perturbation. For each wavelength, we found that, depending on the relative magnitude of the horizontal and vertical component of the perturbation, the mixing layer acquired two distinct modes. Figure 23 shows the two vorticity configurations obtained for a wavelength of 4.15 cm. Figure 23(*a*) shows the '180° out-of-phase' case where the spanwise vortices acquire an undulation in phase with the indentations of the plate. Figure 23(*b*) corresponds to the 'in-phase' case where the spanwise vortices develop an undulation 180° phase shifted with respect to the indentations. The two vorticity modes for the case of perturbations with wavelengths equal to 3.1 cm are given in figure 24. In both figures 23 and 24, the positions of the tips of the indentations have been marked with white dashed lines to show that configuration (*b*) can be obtained by simply shifting the flow configuration (*a*) half a wavelength in the Z-direction.

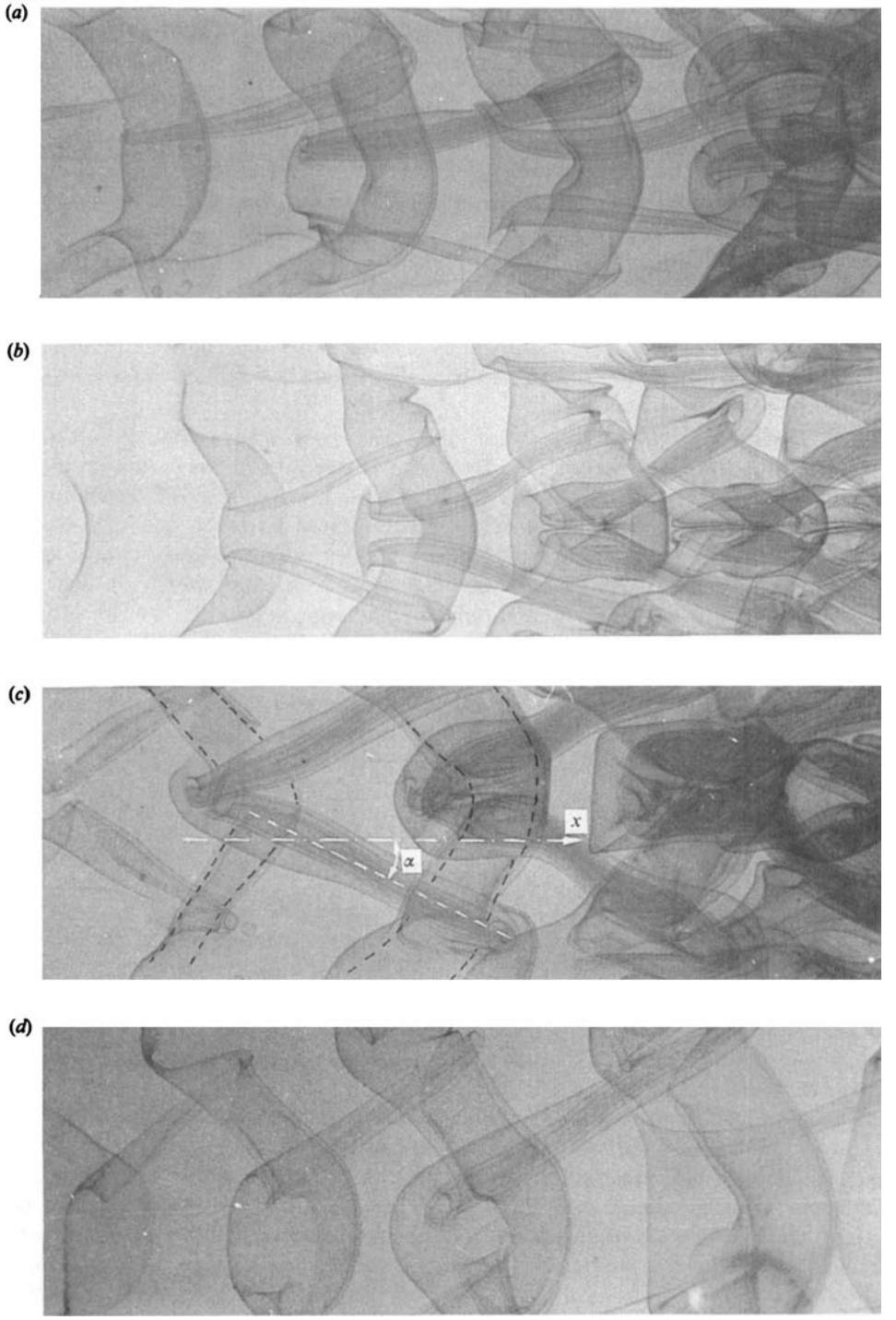

FIGURE 25. Effect of the orientation of the strain field.

6. Effect of the orientation of the strain field

To further analyse the above described strain-driven instability, we conducted additional experiments in which the base-flow was not periodically perturbed along the span, but rather was intentionally modified to lose its two-dimensionality, i.e. the two laminar flow streams were generated with a slightly unequal velocity profile along the span. Because of the resulting uneven distribution of the shear along the span, the strength and the convective velocity of the spanwise vortices formed through the Kelvin–Helmholtz instability were not uniform along the Z-direction. Thus, the spanwise vortex tubes exhibited bends in their axes. Consequently, in this case, the direction of the maximum positive strain field between two consecutive spanwise vortices did not coincide with the streamwise (x) direction. As a result of this, the vortex tubes produced from the stretching of the perturbation component did not have their axes oriented in the flow direction, but rather, in the principal direction of the positive strain field.

Figure 25 shows four top views of different cases where the base-flow was intentionally modified to create a slightly unequal strength in the spanwise vortices along the span. Observe that now as the spanwise vortices exhibit bends in their cores, the direction of maximum positive strain created by them does not coincide with the axial X-direction. In figure 25(c), both the spanwise vortex tubes and the direction of maximum positive strain are indicated. Note that the strain generated by the vortex tubes is oriented in directions at large angles (α) to the axial X-direction. Although attributing their origin to a different flow phenomenon, Thorpe (1987) has also observed the formation of the same type of 'knots' (as he described them) forming between the primary vortices and the non-axial secondary ones.

In conclusion, it seems perhaps more appropriate to call these strain created vortex tubes 'Strain-oriented vortex tubes' rather than 'streamwise vortices' or 'axial vortices' as we have done in the past.

7. Analysis of the 'naturally' developed flow

After having studied the base two-dimensional flow subjected to controlled perturbations periodically placed along the span, we will now analyse the so-called 'natural' case where the base-flow is subjected to uncontrolled small random disturbances.

When the two-dimensional base-flow is left to develop its instabilities 'naturally', the presence of these random disturbances eventually leads to the development of the three-dimensional structure. Figures 26(a) and 26(b) show two plan views of the interface using DIV corresponding to the 'natural' development of the different flow structures. Observe first that since the base-flow originates from two laminar streams having a constant velocity profile (along the span), the vortex tubes which form through the primary shear instability have their axes perpendicular to the flow direction. These spanwise vortex tubes create a streamwise (axial) oriented, positive strain field on the braids. Under the effect of this strain field, the random vorticity perturbations initially present upstream are stretched in the axial direction, eventually resulting in 'streamwise vortex tubes'. Observe in the top views of figure 26 that these vortex tubes are first noticeable on the braids between spanwise vortices and that they further interact with the spanwise vortex tubes causing the appearance of a wavy undulation in the spanwise vortices. (Breidenthal (1981) first observed the formation of these wavy undulations in the spanwise vortex tubes and described them as a 'wiggle').

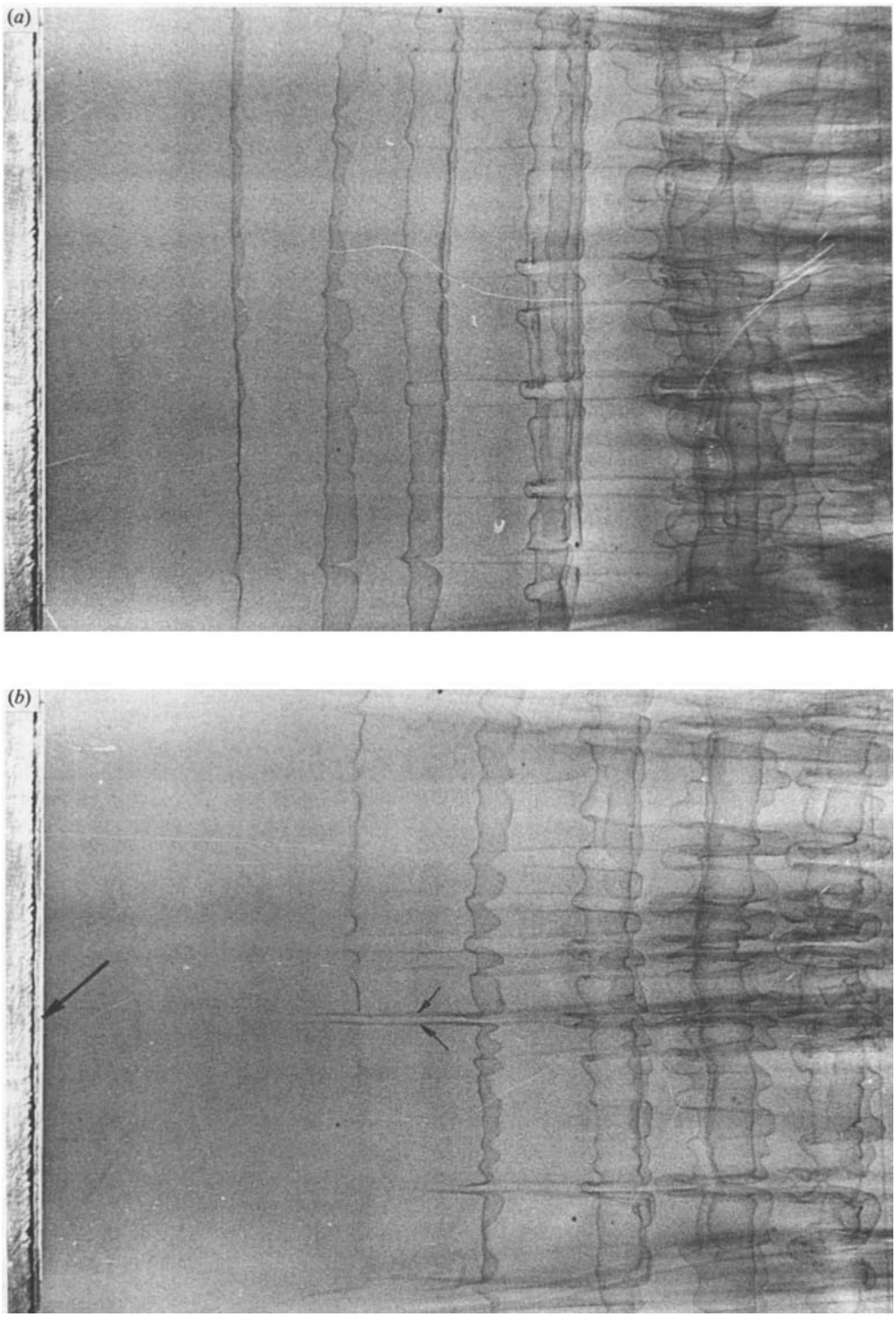

FIGURE 26. (*a*) 'Naturally' developed three-dimensional flow. (*b*) Additional 'localized' perturbation introduced at the position marked by arrow.

In figure 26(*b*) we show the case where, in addition to the random uncontrolled perturbation, a small localized disturbance of the type used in Lasheras *et al.* (1986) was added to the same base-flow. Note that along with the streamwise vortices which were observed forming before, it can now be seen that the localized perturbation has resulted in a pair of closely spaced, small-wavelength, counter-rotating axial vortices (marked in the figure by an arrow). However, note also that the localized perturbation has induced the formation sideways of streamwise vortex tubes. This lateral propagation is a result of the vortex induction combined with the stretching existing in the braids, an effect described by Lasheras *et al.* (1986).

In summary, the cause of the formation of the streamwise vortices in the 'naturally' developing shear layer, is the mutual induction of the perturbed vortices combined with the stretching existing in the braids. Through the analysis of the response of the free shear layer to sinusoidal perturbations distributed along the span, we have not been able to identify the existence of a 'most' unstable wavelength. The question of the possible existence of a preferential spanwise spacement between the axial vortices still remains open. The contribution which this streamwise vortical structure makes to the process of entrainment and interfacial surface generation still remains to be quantified. However, it can be said that, depending on the location and the nature of the upstream disturbances, the scale and position of the axial vortices can vary. Consequently, the pattern of interfacial surface generation and/or entrainment may be substantially affected by the early formation of the three-dimensional structure. By being able to control the location and strength of the axial vortical structure, we will then be able to control the interfacial surface generation throughout the layer. This control of the generation of interfacial surfaces has great potential for many practical applications, i.e. chemical reactors and combustors. Currently, through digital image-processing, three-dimensional analysis of plane free shear layers, we are quantifying the effect of the streamwise vortical structure on entrainment and interfacial surface generation. Comparisons between the base two-dimensional flow and the perturbed one under the effect of the periodically distributed disturbances of the type analysed here will help us understand the effects of the amplitude, wavelength, and type of perturbation on these important parameters of the mixing layer.

8. Conclusion

We have presented a flow-visualization study of the three-dimensional evolution of a plane free shear layer subjected to a single-wave spanwise perturbation in its initial conditions. The qualitative evolution of the layer was observed to consist of the following sequence. First, the two-dimensional shear instability develops forming concentrated regions of almost two-dimensional spanwise vortex tubes. Secondly, under the effect of the positive strain created by the spanwise vortex tubes, the weak perturbed vorticity existing on the braids is stretched, leading to the formation of vortex tubes whose axes align with the direction of maximum positive strain. During this stretching process, the spanwise vortex tubes maintain to a great extent their two-dimensionality, thus suggesting an almost uncoupled development of both instabilities. Thirdly, coupling effects begin to occur whereby the vortex tubes formed through this convective instability further interact with the spanwise vortex tubes inducing on their axes a wavy undulation of the same wavelength, but phase shifted 180° with respect to the perturbation. Fourthly, the vorticity in the layer organizes in a complex topography of vortex tubes composed of an array of spanwise

vortices tangled with the counter-rotating pairs of axial vortices. Finally, this complex vorticity field further develops additional instabilities such as pairings, tearing, and amalgamation among the spanwise vortex tubes, and a much more complicated topography of the vorticity field is achieved.

For the relatively long wavelength of our spanwise perturbations, we did not observe a range of maximum amplification, suggesting that the three-dimensional instability has a long bandwidth for which the amplitudes grow at a comparable rate.

Numerous discussions with Dr Eckart Meiburg have been most valuable in the analysis of the experiments reported here. Comparison of our work to the three-dimensional free shear-layer vortex-dynamics calculations of Ashurst & Meiburg has been useful in interpreting our experimental results. Conversations with Professor Tony Maxworthy have provided constant, stimulated thinking; in particular, regarding the nonlinear interaction between the different vortical structures. Discussions with Professors Frederick Browand and Gilles Corcos have also been most helpful in clarifying some of the ideas expressed in this work.

REFERENCES

Ashurst, W. T. & Meiburg, E. 1988 Three-dimensional shear layers via vortex dynamics. *J. Fluid Mech.* **189**, 87.

Bernal, L. P. 1981 The coherent structure of turbulent mixing layers. PhD dissertation. California Institute of Technology.

Bernal, L. P., Breidenthal, R., Brown, G. L., Konrad, J. H. & Roshko, A. 1981 On the development of three-dimensional small scales in turbulent mixing layers. *Proc. 2nd Symp. Turbulent Shear Flows*, p. 305. August. Berlin.

Breidenthal, R. 1978 A chemically reacting turbulent shear layer. PhD dissertation. California Institute of Technology.

Breidenthal, R. 1980 Response of plane shear layers and wakes to strong three dimensional disturbances. *Phys. Fluids* **23**, 1929.

Breidenthal, R. 1981 Structure in turbulent mixing layers and wakes using a chemical reaction. *J. Fluid Mech.* **109**, 1.

Browand, F. K. & Troutt, T. R. 1980 A note on spanwise structure in the two-dimensional mixing layer. *J. Fluid Mech.* **97**, 771.

Brown, G. L. & Roshko, A. 1971 The effect of density difference on the turbulent mixing layer. *AGARD Conf. Proc.* 93, 23-1-23-11.

Brown, G. L. & Roshko, A. 1974. On density effects and large structure in turbulent mixing layers. *J. Fluid Mech.* **64**, 775.

Corcos, G. M. 1979 The mixing layer: deterministic models of a turbulent flow. *U.C. Berkeley, Mech. Engng Rep.* FM-79-2.

Corcos, G. M. & Lin, S. J. 1984 The mixing layer: deterministic models of a turbulent flow. Part 2. The origin of the three-dimensional motion. *J. Fluid Mech.* **139**, 67.

Corcos, G. M. & Sherman, F. S. 1984 The mixing layer: deterministic models of aturbulent flow. Part 1. Introduction and the two-dimensional flow. *J. Fluid Mech.* **139**, 29.

Dewey, C. F. 1976 Qualitative and quantitative flow field visualization using laser induced fluorescence. *AGARD Conf. Proc.* 193. 17-1-17-7.

Dimotakis, P. & Brown, G. L. 1976 The mixing layer at high Reynolds number: large structure dynamics and entrainment. *J. Fluid Mech.* **78**, 535.

Hama, F. R. 1963 Progressive deformation of a perturbed line vortex filament. *Phys. Fluids* **6**, 526.

Jimenez, J. 1983 A spanwise structure in the shear layer. *J. Fluid Mech.* **132**, 319

JIMENEZ, J., COGOLLOS, M. & BERNAL, L. P. 1985 A perspective view of the plane mixing layer. *J. Fluid Mech.* **152**, 125.

KONRAD, J. H. 1976 An experimental investigation of mixing in two dimensional turbulent shear flows with applications to diffusion limited chemical reachings. *Tech. Rep.* CIT-9-PU.

LASHERAS, J. C., CHO, J. S. & MAXWORTHY, T. 1986 On the origin and evolution of streamwise vortical structures in a plane free shear-layer. *J. Fluid Mech.* **172**, 123.

LASHERAS, J. C. & MAXWORTHY, T. 1987 Structure of the vorticity field in a plane, shear layer.In *Turbulent Shear Flows* (ed. F. Durst, vol. 5, p. 124. Springer.

LIN, S. J. & CORCOS, G. M. 1984 The mixing layer: deterministic models of a turbulent flow. Part 3. The effect of a plane strain on the dynamics of streamwise vortices. *J. Fluid Mech.* **141**, 139.

MEIBURG, E. & LASHERAS, J. C. 1988 Experimental and numerical investigation of the three-dimensional transition in plane wakes. *J. Fluid Mech.* **190**. 1.

METCALFE, R. W., ORSZAG, S. A., BRACHET, M. E., MENON, S. & RILEY, J. J. 1987 Secondary instability of a temporary growing mixing layer. *J. Fluid Mech.* **184**, 207.

NEU, J. C. 1984 The dynamics of stretched vortices. *J. Fluid Mech.* **143**, 253.

OGUCHI, H. & INOUE, O. 1984 Mixing layer produced by a screen and its dependence on initial conditions. *J. Fluid Mech.* **142**, 217.

PIERREHUMBERT, R. T. & WIDNALL, S. E. 1982 The two- and three-dimensional instabilities of a spatially periodic shear layer. *J. Fluid Mech.* **114**, 59.

REBOLLO, M. 1973 Analytical and experimental investigation of a turbulent mixing layer of different gases in a pressure gradient. PhD thesis. California Insitute of Technology.

ROSHKO, A. 1980 The plane mixing layer flow visualization results and three-dimensional effects. In *Proc. Intl Conf. on the Role of Coherent Structures in Modelling Turbulence and Mixing* (ed. J. Jimenez). Lecture Notes in Physics, vol. 136. Springer.

THORPE, S. A. 1987 Transition phenomena and the development of turbulence in stratified fluids: a review. *J. Geophys. Res.* **92**, 5.231.

WINANT, C. D. & BROWAND, F. K. 1974 Vortex pairing: the dynamics of turbulent mixing layer growth at moderate Reynolds number. *J. Fluid Mech.* **63**, 237.

WYGNANSKI, I., OSTER, D., FIEDLER, H. & DZIOMBA, B. 1969 On the perseverance of a quasi-two-dimensional eddy-structure in a turbulent mixing layer. *J. Fluid Mech.* **93**, 325.